LANDSCAPE ANALYSIS OF EXCITED STATES CALCULATION OVER QUANTUM COMPUTERS

HENGZHUN CHEN[*], YINGZHOU LI[†], BICHEN LU[‡], AND JIANFENG LU[§]

Abstract. The variational quantum eigensolver (VQE) is one of the most promising algorithms for low-lying eigenstates calculation on Noisy Intermediate-Scale Quantum (NISQ) computers. Specifically, VQE has achieved great success for ground state calculations of a Hamiltonian. However, excited state calculations arising in quantum chemistry and condensed matter often requires solving more challenging problems than the ground state as these states are generally further away from a mean-field description, and involve less straightforward optimization to avoid the variational collapse to the ground state. Maintaining orthogonality between low-lying eigenstates is a key algorithmic hurdle. In this work, we analyze three VQE models that embed orthogonality constraints through specially designed cost functions, avoiding the need for external enforcement of orthogonality between states. Notably, these formulations possess the desirable property that any local minimum is also a global minimum, helping address optimization difficulties. We conduct rigorous landscape analyses of the models' stationary points and local minimizers, theoretically guaranteeing their favorable properties and providing analytical tools applicable to broader VQE methods. A comprehensive comparison between the three models is also provided, considering their quantum resource requirements and classical optimization complexity.

Key words. Variational quantum eigensolver, excited states calculation, landscape analysis, oblique manifold

1. Introduction. With the availability of near-term quantum devices and significant advancements in quantum supremacy experiments [2, 45], quantum computing has gained substantial attention from various scientific disciplines in recent years. Algorithms designed for these restricted devices, known as noisy intermediate-scale quantum (NISQ) devices [34], have distinct characteristics: they operate on a small number of qubits, exhibit some level of noise resilience, and often employ hybrid approaches that combine quantum and classical computing steps. An example is the variational quantum eigensolver (VQE) [27, 33], which shows particular promise within the NISQ paradigm.

In general, VQE aims to variationally determine an upper bound to the ground state energy of a Hamiltonian, which enables important energetic predictions for molecules and materials [9]. Namely, given a Hamiltonian $\hat{H}$ with any normalized trial wavefunction $|\psi\rangle$, the ground state energy E_0 associated with $\hat{H}$ is bounded by $E_0 \leq \langle\psi|\hat{H}|\psi\rangle$. The goal of VQE is to find a parametrization of $|\psi\rangle$ such that the expectation value of $\hat{H}$ is minimized. Note that the normalized trial wavefunction $|\psi\rangle$ over a quantum computer is implemented by $\hat{U}(\theta)|0\rangle$, where $\hat{U}(\theta)$ is a parameterized unitary operation. We can rewrite the VQE optimization problem with corresponding cost function as

$$E_{\text{VQE}} = \min_{\theta} \ \langle 0|\hat{U}^{\dagger}(\theta)\hat{H}\hat{U}(\theta)|0\rangle.$$

The hybrid nature of VQE arises from the fact that the expectation value can be

[*]School of Mathematical Sciences, Fudan University (hengzhunchen21@m.fudan.edu.cn).

[†]School of Mathematical Sciences, Shanghai Key Laboratory for Contemporary Applied Mathematics, Fudan University and Key Laboratory of Computational Physical Sciences, Ministry of Education (yingzhouli@fudan.edu.cn).

[‡]Shanghai Center for Mathematical Sciences, Fudan University (bclu18@fudan.edu.cn).

[§]Department of Mathematics, Department of Physics and Department of Chemistry, Duke University (jianfeng@math.duke.edu).

computed on a quantum device while the minimization problem with respect to θ is computed on a classical computer.

Compared to other quantum eigensolvers, such as quantum phase estimation (QPE) [1, 3, 18], which require circuit depths far beyond the capabilities of near-term intermediate-scale quantum (NISQ) devices, the variational quantum eigensolver (VQE) offers a more NISQ-friendly approach. VQE relies on shorter circuit depths and fewer qubits but comes at the cost of increased number of measurements, parameter optimization on a classical computer and the need for a predefined ansatz to approximate eigenstates. The choice of an appropriate ansatz is a critical component of the VQE workflow and has been the focus of significant research in recent years.

The hardware-efficient ansatz (HEA) [17] directly parameterizes quantum states using native quantum gates, making it well-suited for certain problem-specific scenarios. However, it is often inadequate for large-scale chemical problems due to its limited scalability. In contrast, the unitary coupled cluster (UCC) ansatz [33], along with its extensions such as UCCSD [35], UCCGSD [19], and k-UpCCGSD [19], has demonstrated strong numerical accuracy with only linear scaling in quantum resource requirements. This makes UCC-based ansatzes a promising trade-off between computational cost and accuracy. Recent studies [12, 36] have also explored adaptive ansatz structures, which allow the ansatz dimensions to vary dynamically. These approaches aim to provide reliable alternatives or improvements over fixed-structure ansatzes, further enhancing VQE's flexibility and efficiency.

A promising application for VQE is ab initio electronic structure calculation. In particular, VQE solves the many-body problem under the full configuration interaction (FCI) framework [6, 14, 20, 40, 43], where the time-independent Schrödinger equation is discretized exactly and the ground state is computed by solving the standard eigenvalue problem exponential-scaling with the number of electrons in the system. The exponential cost of classical FCI fits well with capabilities of quantum algorithms. Accordingly, quantum algorithms for ground state calculation under the FCI framework have been extensively explored over recent decades [1, 3, 4, 25, 33]. Among them, VQE is a quantum-classical hybrid approach with the shortest circuit depth, which makes it the most widely applied quantum eigensolver on NISQ devices.

In addition to the ground state, the consideration of excited states is also crucial in quantum chemistry. However, computing excited states is generally a more challenging task, due to the excited states generally being further away from a mean-field description, as well as less straightforward optimization to avoid the variational collapse to the ground state. Existing quantum algorithms for excited states computation can be broadly divided into two main types of methods: the perturbation-based approaches and the variational approaches.

Perturbation-based methods always start from the ground state via VQE and then evaluate the expansion values on single excited states from the ground state. With these expansion values they further utilize different approaches to obtain the low-lying excited state energies. The representatives in this category could be the quantum subspace expansion (QSE) method [8, 10, 26] and quantum equation of motion (qEoM) [30].

For the variational approach, it uses modified VQE cost functions to afford a fully variational flexibility and maintain the orthogonality of the low-lying eigenstates. These methods have the advantage of avoidance for the limitations and biases of perturbation-based methods, but usually come with a higher cost of quantum resources and the restriction to a specific ansatz chosen. For instance, the folded spectrum method [27] folds the spectrum of a Hamiltonian operator via a shift-and-

square operation, i.e., $\hat{H} \to (\hat{H} - \lambda I)^2$, where λ is a chosen number and as such the ground state of $(\hat{H} - \lambda I)^2$ is the eigenstate of $\hat{H}$ whose eigenvalue is closest to λ. Then $(\hat{H} - \lambda I)^2$ is used as the Hamiltonian operator in VQE to obtain the desired excited states. The witness-assisted variational eigenspectra solver [38, 39] incorporates an entropy term in the objective function to prevent variational collapse back to the ground state by requiring the minimized excited state to be close to its initial state, which is defined as an excitation from the ground state. The quantum deflation method [13, 16] adopts the overlapping term between the target state and the ground state as a penalty term in the objective function to keep the target state as orthogonal as possible to the ground state.

While the methods above all have their classical algorithm counterpart, two methods, subspace search VQE (SSVQE) [28] and multistate contracted VQE (MCVQE) [32] leverage a unique property of quantum computing to maintain the orthogonality between eigenstates: all quantum operations are unitary and a unitary transformation will not change the orthogonality of the states it is applied to. They first prepare K non-parameterized mutually orthogonal states $|\phi_1\rangle, |\phi_2\rangle, \ldots, |\phi_K\rangle$ and then apply a parameterized unitary circuit $\hat{U}_\theta$ to these states. Hence, we can minimize the objective function

$$\sum_{k=1}^{K} \langle \phi_k | \hat{U}_\theta^\dagger \hat{H} \hat{U}_\theta | \phi_k \rangle,$$

to obtain the desired eigenstates simultaneously. However, energies associated with $\hat{U}_\theta |\phi_1\rangle, \ldots, \hat{U}_\theta |\phi_K\rangle$ may not be ordered. Hence, SSVQE introduces a min-max problem to obtain a specific excited state and a weighted objective function to preserve the ordering of eigenstates in some further extensions. Instead, MCVQE uses a classical post-processing to extract the ordered eigenstates from the eigen-subspaces obtained from the optimization procedure. Specifically, it gives the approximated eigenstates in the form of $|\psi_k\rangle = \sum_l \hat{U}_\theta |\phi_l\rangle V_{lk}$, where V_{lk} is the (l,k)-th entry of a unitary matrix V, which is the eigenvector matrix of the entangled contracted Hamiltonian $H_{kl} := \langle \phi_k | \hat{U}_\theta^\dagger \hat{H} \hat{U}_\theta | \phi_l \rangle$.

As discussed, maintaining orthogonality between low-lying eigenstates is a central algorithmic challenge for excited state computations, regardless of whether orthogonality constraints are addressed explicitly or implicitly. Motivated by the quantum orbital minimization method (qOMM) [5], in this work we will theoretically analyze several approaches that embed the orthogonality constraints into the cost function itself, resulting in an "unconstrained optimization" that fits better to the quantum computer. Specifically, we obtain the energy landscape of these methods (including the qOMM), which provides theoretical guarantees for the favorable properties of the corresponding quantum algorithms.

Now we give the mathematical formulation of the excited states quantum eigensolver problem in matrix notation for later discussion. Given Hermitian matrix $A \in \mathbb{C}^{n \times n}$, our target is to find the smallest p eigenpairs of A, denoted as

$$AX = X\Lambda, \quad X \in \mathbb{C}^{n \times p},$$

where Λ is the diagonal eigenvalue matrix. In the quantum computing setting, each column of X is represented by ansatz like $|\psi_i\rangle = \hat{U}_{\theta_i} |\phi_i\rangle$ with $\hat{U}_{\theta_i}$ being a unitary operator for $i = 1, \ldots, p$. If quantum error is not taken into account, each column of X will always be of unit length, which gives the constraints for diagonal elements of

X^*X. Further, this constraint corresponds to the oblique manifold, which is defined as [1]

$$\mathcal{OB}(n,p) = \left\{ X \in \mathbb{C}^{n \times p} : \operatorname{diag}(X^*X) = \mathbf{1} \right\}, \tag{1.1}$$

where $\mathbf{1}$ denotes an all-one vector of length p. Thus, we emphasize that although we apply the unconstrained optimization problem over a quantum computer, the quantum computer itself puts the extra oblique manifold constraints to the optimization problem due to the normality condition of any quantum state. Moreover, we remark that since the representability of ansatz circuit is typically sufficient, i.e., the variational space is rich enough, especially for the chemical systems, we ignore the ansatz design and investigate the energy landscape of VQE cost function with respect to $X \in \mathcal{OB}(n,p)$ directly.

Consider the well known optimization formulation of classical eigensolver, [2]

$$\min_{X \in \mathbb{C}^{n \times p}} \operatorname{tr}(X^*AX), \quad \text{s.t.} \quad X^*X = I_p.$$

To address the orthogonal constraints for excited states computation, we introduce the three models below as examples; each provides a method to embed the orthogonality constraint into the objective function, while the oblique manifold constraint arises from the nature of quantum computers,

$$\text{(qOMM)} \qquad \min_{X \in \mathcal{OB}(n,p)} \operatorname{tr}\left((2I - X^*X)X^*AX \right),$$

$$\text{(qTPM)} \qquad \min_{X \in \mathcal{OB}(n,p)} \frac{1}{2}\operatorname{tr}(X^*AX) + \frac{\mu}{4}\left\| X^*X - I \right\|_{\mathrm{F}}^2,$$

$$\text{(qL1M)} \qquad \min_{X \in \mathcal{OB}(n,p)} \operatorname{tr}(X^*AX) + \mu_1 \sum_{i<j} \left| (X^*X)_{ij} \right|,$$

where $\|\cdot\|_{\mathrm{F}}$ denotes the Frobenius norm and $\mu, \mu_1 > 0$ are finite penalty constants. Each objective function above leads to a quantum eigensolver. Additionally, qOMM and qTPM require matrix A to be negative definite Hermitian, while qL1M works for any Hermitian matrix A and requires $p < n$. We note that the first model has been developed as a hybrid quantum-classical algorithm, termed the quantum orbital minimization method (qOMM) [5]. The latter two models (qTPM and qL1M) have their own favorable properties and are promising candidates for VQE algorithms. In this work, we analyze the energy landscape of the proposed models. As the main contribution, we present theorems that characterize the stationary points and local minimizers of all three models. Notably, all three models possess the favorable property that any local minimum is also a global minimum.

The rest of the paper is organized as follows. In section 2, all three models will be investigated in detail. A formal statement, together with their landscape analysis and algorithm frameworks are given. The complete proof of the theorems will be presented in the appendix. In section 3, we present simulated quantum numerical results to demonstrate the convergence of the VQE algorithms. Furthermore, we compare their efficiency in terms of quantum resource requirements and classical optimization complexity. Finally, section 4 concludes the paper and discusses future work.

---

[1]For the sake of notation, we adopt $\operatorname{diag}(\cdot)$ similar to the MATLAB "diag" function, i.e., $\operatorname{diag}(v)$ is a square diagonal matrix with the entries of vector v on the diagonal and $\operatorname{diag}(A)$ is a column vector of the diagonal entries of A.

[2]We use I_p to denote the identity matrix of size p-by-p. For notation simplicity, we also use I to denote the identity matrix with size consistent to the matrix operations.

2. Optimization Landscape and Algorithms in VQE. In this section, we provide a detailed landscape analysis and the algorithm framework of the three proposed formulations. Proofs of the theorems stated here are deferred to the appendix. Specifically, we characterize and contrast properties of stationary points and local minimizers for these formulations. This lays theoretical groundwork for understanding their algorithmic behavior and deriving optimization algorithms.

2.1. qOMM. The original orbital minimization method (OMM) was initially developed to solve for the low-lying eigenspace of a negative definite Hermitian matrix A in Kohn-Sham density functional theory [24, 31]. It employs the energy functional given by

$$E_0(X) = \text{tr}\left((2I - X^*X)X^*AX\right),$$

where X represents a matrix of orbitals. Notably, OMM possesses a few favorable properties [23], which provides some benefits for the algorithm design. First, even though the orthogonality constraint among the columns of X is not explicitly enforced, the minimizers of $E_0(X)$ inherently consist of mutually orthogonal vectors. Second, although the energy functional is non-convex, each local minimum is also a global minimum.

OMM has been generalized over quantum computer as a VQE, and it leads to the qOMM method, where the energy landscape is unknown but numerically performs well. Correspondingly, we aim to characterize the stationary points and local minimizers of qOMM, which are given by the optimization problem:

$$(2.1) \qquad \min_{X \in \mathcal{OB}(n,p)} E_0(X) = \text{tr}\left((2I - X^*X)X^*AX\right).$$

In contrast to the straightforward characterization of stationary points for the unconstrained optimization in OMM, Theorem 2.1 reveals a more intricate structure of the stationary points for qOMM. This subtle result for stationary points can then be leveraged to deduce the desired property of local minimizers stated in Theorem 2.3.

THEOREM 2.1. *Given a negative definite Hermitian matrix A, stationary points of qOMM (2.1) take the form XP, where $P \in \mathbb{R}^{p \times p}$ is an arbitrary permutation matrix, $X \in \mathbb{C}^{n \times p}$ admits a block structure, $X = (X_1, \cdots, X_k)$, and k is the number of blocks. For each block $X_i \in \mathbb{C}^{n \times p_i}$, we denote the reduced SVD as $X_i = U_i\Sigma_i V_i^*$ and the rank as r_i, where $\Sigma_i = \text{diag}(\sigma_{i1}, \ldots, \sigma_{ir_i})$ is the nonzero singular value matrix. Matrix U is composed of column bases of X_is, i.e., $U = (U_1, \cdots, U_k)$. The following conditions hold.*

1. *The matrix U is partial unitary and diagonalize A, i.e., $U^*U = I$ and U^*AU is diagonal.*
2. *Denote the j-th diagonal entry of $U_i^*AU_i$ as $\tilde{a}_{ij}$. Singular values are,*

$$\sigma_{ij} = \sqrt{1 + \frac{p_i - r_i}{\tilde{a}_{ij} \cdot \sum_{\ell=1}^{r_i} \frac{1}{\tilde{a}_{i\ell}}}} \geq 1.$$

   Furthermore, if the j-th column u_{ij} of U_i is not an eigenvector of A, then $\sigma_{ij} = \sqrt{2}$.
3. *At most one block X_i is of full rank, and then $X_i = U_iV_i^*$;*
4. *The right singular vector matrix $V_i \in \mathbb{C}^{p_i \times r_i}$ is partial unitary such that $X_i \in \mathcal{OB}(n, p_i)$. The existence of V_i is guaranteed for any given U_i.*

In addition, any $X \in \mathbb{C}^{n \times p}$ satisfying the conditions above is a stationary point of qOMM (2.1).

The proof of Theorem 2.1 is given in Appendix A.

Remark 2.2. When X_i is full rank, all the columns of U_i are eigenvectors of matrix A. Otherwise U_i may not be eigenvectors. This is very different from OMM without constraint. Here we give a concrete example for illustration. Suppose A is a 7-by-7 negative definite Hermitian matrix with eigendecomposition $A = Q\Lambda Q^*$ where

$$Q = (q_1, \cdots, q_7), \quad \Lambda = \mathrm{diag}(-1, -2, -3, -4, -5, -6, -7).$$

Now we construct a stationary point of size 7-by-5 with rank 2 from its reduced SVD,

$$X = U\Sigma V^* := (q_2, u_2) \begin{pmatrix} \sqrt{3} & \\ & \sqrt{2} \end{pmatrix} V^*, \quad u_2 = \sqrt{\frac{2}{5}} q_1 + \sqrt{\frac{3}{5}} q_6,$$

where $V \in \mathbb{C}^{2 \times 5}$ is partial unitary such that $\mathrm{diag}(X^*X) = \mathbf{1}$. Let $D = -8I$, substitute X into the zero gradient condition (A.4), one could verify that

$$2AX - AXX^*X - XX^*AX + XD = 0,$$

which shows that such X is a stationary point but the second column of U is not an eigenvector of A.

THEOREM 2.3. *Given a negative definite Hermitian matrix A, the local minimizers of qOMM* (2.1) *take the form of $X = Q_p V^*$, where Q_p are eigenvectors of A corresponding to the p smallest eigenvalues, $V \in \mathbb{C}^{p \times p}$ is an arbitrary unitary matrix. Conversely, any matrix in the form of $Q_p V^*$ is a local minimizer of qOMM. Furthermore, any local minimum of qOMM is also a global minimum.*

The proof of Theorem 2.3 is given in Appendix A.

Remark 2.4. Let matrix A have eigenvalues ordered non-decreasingly as $\lambda_1 \leq \lambda_2 \leq \cdots \leq \lambda_n$. The eigenvectors corresponding to the smallest p eigenvalues of A may not be unique if $\lambda_p = \lambda_{p+1}$, leading to degeneracy. In this paper, when we refer to the "smallest p eigenvalues", we include any valid choice of eigenvectors in cases of degeneracy.

From the landscape analysis above, we can observe that all the local minima have the same objective function value and constitute the set of global minima. The minimizers at these local minima consist of mutually orthogonal vectors. This property leads to an algorithm design where explicit orthogonal constraints are not required. Rather, orthogonality of the minimizers can naturally emerge throughout the optimization process without any orthogonalization steps, which allows for greater flexibility in the choice of ansatz applied to each input state and the choice for input states itself.

Given that the algorithm design and numerical experiments have been thoroughly discussed in [5], here we omit the details of the algorithm of qOMM. Note that the algorithm design of qOMM and qTPM are similar; one can also refer to subsection 2.2 for the framework.

2.2. qTPM. It is well known that the invariant subspace associated with the p algebraically smallest eigenvalues of matrix A yields an optimal solution to the trace

minimization problem with orthogonality constraints

$$\min_{X\in\mathbb{C}^{n\times p}} \operatorname{tr}(X^*AX), \quad \text{s.t.} \quad X^*X = I.$$

Thus, we can introduce a penalty term using the Frobenius norm to construct the corresponding unconstrained optimization problem:

$$(2.2) \qquad \min_{X\in\mathbb{C}^{n\times p}} f_\mu(X) := \frac{1}{2}\operatorname{tr}(X^*AX) + \frac{\mu}{4}\|X^*X - I\|_{\mathrm{F}}^2,$$

where the penalty parameter $\mu > 0$ takes suitable finite values. This trace penalty minimization method (TPM) finds the optimal eigenspace and excludes all full-rank non-optimal stationary points for an appropriately chosen μ [11, 44]. This differs from general classical quadratic penalty methods, which require the penalty parameter μ to go to infinity for the penalty model to approach the original constrained model.

Now consider applying the TPM model to the quantum computing setting, which gives the quantum trace penalty minimization method (qTPM), i.e.,

$$(2.3) \qquad \min_{X\in\mathcal{OB}(n,p)} f_\mu(X) = \frac{1}{2}\operatorname{tr}(X^*AX) + \frac{\mu}{4}\|X^*X - I\|_{\mathrm{F}}^2.$$

Note that for X in oblique manifold $\mathcal{OB}(n,p)$, one has

$$\|X^*X - I\|_{\mathrm{F}}^2 = \operatorname{tr}(X^*XX^*X) + \operatorname{tr}(I - 2X^*X) = \operatorname{tr}(X^*XX^*X) - p.$$

Thus, the optimization model (2.3) is equivalent to

$$(2.4) \qquad \min_{X\in\mathcal{OB}(n,p)} g_\mu(X) := \frac{1}{2}\operatorname{tr}(X^*AX) + \frac{\mu}{4}\operatorname{tr}(X^*XX^*X).$$

This formulation gives some flexibility and convenience for theoretical analysis. Consequently, we also refer to it as the qTPM model.

Remark 2.5. With $\mu > 0$ the TPM model (2.2) is equivalent to another useful method for large-scale eigenspace computation called the symmetric low-rank product (SLRP) model [21, 22] defined as

$$\min_{X\in\mathbb{C}^{n\times p}} \frac{1}{2}\|XX^* - A\|_{\mathrm{F}}^2,$$

in the sense that any stationary point of one problem, after scaling and shifting, has a one-to-one correspondence with a stationary point of the other. This equivalence comes from the identity

$$\frac{1}{2}\operatorname{tr}(X^*AX) + \frac{\mu}{4}\|X^*X - I\|_{\mathrm{F}}^2 \equiv \frac{\mu}{4}\left\|XX^* - (I - \frac{A}{\mu})\right\|_{\mathrm{F}}^2 + \text{constant}.$$

Since these two models are equivalent, we only discuss the qTPM, the generalization of SLRP model to the quantum computing setting can be carried out in the same manner.

Now let us analyze the energy landscape of qTPM. While the local minimizers of OMM and qOMM are the same, the explicit penalty term in Frobenius norm leads to a different behavior for TPM and qTPM. Note that local minimizers of TPM are

scaled eigenvectors of matrix A, right multiplying any unitary matrix [44], which does not satisfy the constraint in qTPM. Hence the local minimizers of qTPM are different from that in TPM. Specifically, we have the following results describing the landscape properties of qTPM.

THEOREM 2.6. *Given* $\mu > |\lambda_{\min}(A)|$ *and a negative definite Hermitian matrix* A [3], *stationary points of qTPM* (2.4) *take the form* XP, *where* P *is an arbitrary permutation matrix and* $X = (X_1, \cdots, X_k)$, *where* $X_i \in \mathbb{C}^{n \times p_i}$ *with rank* r_i *for* $i = 1, \ldots, k$. *Denote the singular value decomposition of each* X_i *as* $X_i = U_i \Sigma_i V_i^*$, *where* $U_i \in \mathbb{C}^{n \times p_i}$, $\Sigma_i \in \mathbb{R}^{p_i \times p_i}$, $V_i \in \mathbb{C}^{p_i \times p_i}$. *Let*

$$U = (U_1, \cdots, U_k), \quad \Sigma = \mathrm{diag}\,(\Sigma_1, \cdots, \Sigma_k), \quad V = \mathrm{diag}\,(V_1, \cdots, V_k),$$

we have $X = U\Sigma V^*$, *such* X *satisfies the following conditions:*
   1. $U^*U = I$, *each* U_i *consists of eigenvectors of* A *with eigenvalues* $\lambda_{i1}, \ldots, \lambda_{ip_i}$ *for* $i = 1, \ldots, k$.
   2. *For* $i = 1, \ldots, k$, $\Sigma_i = \mathrm{diag}\,(\sigma_{i1}, \cdots, \sigma_{ip_i})$ *with*

$$\sigma_{ij} = \sqrt{\frac{p_i}{r_i} - \frac{1}{\mu}\left(\lambda_{ij} - \frac{1}{r_i}\sum_{l=1}^{r_i}\lambda_{il}\right)},$$

   for $j = 1, \ldots, r_i$; $\sigma_{ij} = 0$, $j = r_i + 1, \ldots, p_i$.
   3. $V^*V = I$, *each* $V_i \in \mathbb{C}^{p_i \times p_i}$ *is unitary such that* $X_i \in \mathcal{OB}(n, p_i)$ *for* $i = 1, \ldots, k$.
Besides, any $X \in \mathbb{C}^{n \times p}$ *satisfying the conditions above is a stationary point of qTPM* (2.4).

THEOREM 2.7. *Local minimizers of qTPM* (2.4) *with* $\mu > |\lambda_{\min}(A)|$ *and negative definite Hermitian matrix* A *take the form of*

$$(2.5) \qquad X = Q_p(I - \frac{1}{\mu}(\Lambda_p - \bar{\Lambda}_p))^{1/2}V^*, \quad \bar{\Lambda}_p = \frac{1}{p}\mathrm{tr}(\Lambda_p)I,$$

where Q_p *are eigenvectors of* A *corresponding to the* p *smallest eigenvalues* Λ_p *(counting geometric multiplicity)*, $V \in \mathbb{C}^{p \times p}$ *is unitary matrix such that* $\mathrm{diag}(X^*X) = \mathbf{1}$. *Conversely, any matrix in the form* (2.5) *is a local minimizer of qTPM. Furthermore, any local minimum of qTPM is also a global minimum.*

The proofs of Theorem 2.6 and Theorem 2.7 are given in Appendix B.

From the landscape analysis above, we can also observe that all the local minima have the same objective function value and constitute the set of global minima. Although the local minimizers of qTPM have a more intricate structure than qOMM, they nonetheless encode the target eigen-subspace associated with the p smallest eigenvalues of matrix A (counting for geometric multiplicity). Through a post-processing procedure such as Rayleigh-Ritz projection, the final eigenpair approximations can be extracted. Thus, qTPM successfully captures the pertinent eigen-information at its minimizers, even if not in the simplest form prior to post-processing.

We now present an algorithm framework for qTPM. In the quantum computing setting of qTPM, each column of X is represented by the ansatz $|\psi_i\rangle = \hat{U}_{\theta_i}|\phi_i\rangle$ for

---

[3]We use $\lambda_{\min}(\cdot)$ and $\lambda_{\max}(\cdot)$ to denote the minimum and maximum eigenvalues of a matrix respectively.

$i = 1, \ldots, p$, where $|\phi_1\rangle, \ldots, |\phi_p\rangle$ are initial states, $\hat{U}_{\theta_1}, \ldots, \hat{U}_{\theta_p}$ are parameterized circuits with $\theta_1, \ldots, \theta_p$ being parameters. Thus, our objective function and optimization problem (2.4) turn into

$$\min_{\theta_1, \cdots, \theta_p} \quad \frac{1}{2}\sum_{i=1}^{p}\langle\phi_i|\hat{U}_{\theta_i}^{\dagger}\hat{H}\hat{U}_{\theta_i}|\phi_i\rangle + \frac{\mu}{2}\sum_{i,j=1, i<j}^{p}\left|\langle\phi_i|\hat{U}_{\theta_i}^{\dagger}\hat{U}_{\theta_j}|\phi_j\rangle\right|^2,$$

where $\hat{H}$ is the Hamiltonian operator of the system. Given this variational formulation, one can construct quantum circuits to evaluate both inner products appearing in the objective function above, i.e., $\langle\psi_i|\hat{H}|\psi_j\rangle$ and $\langle\psi_i|\psi_j\rangle$ respectively. When the evaluation of the objective function is available, we can adopt a gradient-free optimizer to minimize the objective function with respect to parameters $\theta_1, \ldots, \theta_p$. After the optimization process, we obtain a set of parameters such that $\hat{U}_{\theta_1}|\phi_1\rangle, \ldots, \hat{U}_{\theta_p}|\phi_p\rangle$ approximate the target eigenspace $Q_p S$, where $Q_p \in \mathbb{C}^{n\times p}$ are p eigenvectors of $\hat{H}$ associated with the smallest p eigenvalues and $S \in \mathbb{C}^{p\times p}$ is an invertible matrix. Thus we can perform a Rayleigh-Ritz step to extract the desired eigenspace. Specifically, we construct two matrices, B and C, with their (i,j)-th elements defined as follows:

$$B_{ij} = \langle\phi_i|\hat{U}_{\theta_i}^{\dagger}\hat{H}\hat{U}_{\theta_j}|\phi_j\rangle \quad \text{and} \quad C_{ij} = \langle\phi_i|\hat{U}_{\theta_i}^{\dagger}\hat{U}_{\theta_j}|\phi_j\rangle.$$

We then solve a generalized eigenvalue problem with the matrix pencil (B, C), given by:

$$BR = CR\Lambda,$$

where R represents the eigenvector matrix, and Λ is a diagonal matrix with the eigenvalues of (B, C) as its diagonal entries. Finally, we obtain the desired eigenvalues contained in Λ, along with the corresponding eigenvectors $\sum_{j=1}^{p}\hat{U}_{\theta_j}|\phi_j\rangle R_{ji}$ for $i = 1, \ldots, p$.

2.3. qL1M. In addition to the Frobenius norm penalty, we could also consider other types of penalty like the l_1 penalty, which gives the quantum l_1 minimization method (qL1M),

$$(2.6) \qquad \min_{X\in\mathcal{OB}(n,p)} E_1(X) := \mathrm{tr}(X^*AX) + \mu_1\sum_{i<j}\left|(X^*X)_{ij}\right|,$$

with $\mu_1 > 0$ taking an appropriate value. Despite the nonsmooth nature of the objective function introduced by the l_1 penalty term, desirable properties can be established due to its well-known "exactness" property [29]. Specifically, given the penalty parameter larger than a certain value, solving the unconstrained problem with respect to X yields the exact solution to the original constrained problem. We now proceed to identify the local minimizers for a detailed characterization of the landscape of qL1M.

THEOREM 2.8. *Local minimizers of qL1M* (2.6) *for Hermitian matrix A with $\mu_1 > 16p\|A\|_2$ and $p < n$ take the form $X = Q_p V^*$, where $V \in \mathbb{C}^{p\times p}$ is an arbitrary unitary matrix and Q_p consists of eigenvectors of the p smallest eigenvalues of A (counting geometric multiplicity). Conversely, any matrix in the form of $Q_p V^*$ is a local minimizer of qL1M. Furthermore, any local minimum of qL1M is also a global minimum.*

The proof of Theorem 2.8 is given in Appendix C.

Note that large-scale eigenvalue problems typically aim to find only a few most important eigenpairs. Hence, the constraint $p < n$ in Theorem 2.8 is acceptable in practice.

The theorem above demonstrates that the local minimizers of the qL1M exhibit the same elegant structure as qOMM. Similarly, orthogonality of the minimizers can naturally emerge throughout the optimization process without any orthogonalization steps. This favorable structure indicates the prospects for deriving computationally efficient algorithms for qL1M that leverage established l_1 regularization techniques.

Remark 2.9. Consider the weighted form of qL1M, which is defined as

$$(2.7) \qquad \min_{X \in \mathcal{OB}(n,p)} \operatorname{tr}(X^*AXW) + \mu_1 \sum_{i<j} |(X^*X)_{ij}|,$$

where weighted matrix $W = \operatorname{diag}(w_1, \cdots, w_p)$ such that $w_1 > w_2 > \cdots > w_p > 0$. One can easily verify that the proof of Theorem 2.8 can be applied to the weighted qL1M (2.7) and we conclude that the local minimum of (2.7) with $\mu_1 > 0$ sufficiently large must be the local minimum of

$$\min_{X \in \mathbb{C}^{n \times p}} \operatorname{tr}(X^*AXW), \quad \text{s.t.} \quad X^*X = I.$$

Therefore, we have local minimizer $X = Q_p$ for the weighted qL1M, where Q_p are ordered eigenvectors corresponding to the p smallest eigenvalues of A (counting geometric multiplicity).

Now let us briefly discuss the algorithm design for the qL1M. In the quantum computing setting of qL1M, our objective function and optimization problem (2.6) turn into

$$\min_{\theta_1, \cdots, \theta_p} \quad \sum_{i=1}^{p} \langle \phi_i | \hat{U}_{\theta_i}^\dagger \hat{H} \hat{U}_{\theta_i} | \phi_i \rangle + \mu_1 \sum_{i,j=1,i<j}^{p} \left| \langle \phi_i | \hat{U}_{\theta_i}^\dagger \hat{U}_{\theta_j} | \phi_j \rangle \right|,$$

where $\hat{H}$ is the Hamiltonian operator of the system. Starting from this objective function and following the same steps as qTPM, the desired eigenpairs can be obtained. Additionally, more powerful and efficient optimization algorithms could be developed by utilizing advanced techniques for handling the l_1 penalty, though this lies beyond the scope of this paper. The nonsmooth nature of the problem presents opportunities for novel algorithm designs tailored to the qL1M formulation, offering an interesting direction for future research.

3. Numerical Results. In this section, we conduct a comparative analysis of the three VQE models: qOMM, qTPM, and qL1M, to assess their practical performance. The comparison is twofold: we first evaluate the quantum resource cost associated with each model, and then we present numerical simulations to investigate their optimization behavior and convergence. These results provide empirical validation for our theoretical findings and clarify the trade-offs between the different approaches to enforce orthogonality.

3.1. Quantum resource estimate. We first analyze the efficiency of the three VQE models by comparing their quantum resource costs. We begin with the quantum circuits used to evaluate state inner products. For two states $|\psi\rangle = \hat{U}_\psi |0\rangle$ and $|\phi\rangle =$

$\hat{U}_\phi|0\rangle$, the complex-valued inner product $\langle\psi|\phi\rangle$ could be evaluated via the extended Hadamard test [5], which computes the real and imaginary parts separately with two circuits. In contrast, the real-valued fidelity $|\langle\psi|\phi\rangle|^2$ could be measured with only one circuit, for instance, the inversion test (measuring overlap $\langle 0|U_\psi^\dagger U_\phi|0\rangle$) or the SWAP test. While other variants exist, for the small qubit systems considered here, these circuits are broadly comparable in depth and qubit count. We therefore focus our analysis on the number of inner product test circuits in each model, which is a primary indicator of both circuit execution time and overall quantum resource expenditure.

The evaluation of the objective function of our VQE models involves two parts: the Hamiltonian part and the regularization part. Assume that the Hamiltonian $\hat{H}$ is decomposed into a linear combination of N_U Hermitian and unitary operators (e.g., Pauli strings) as $\hat{H} = \sum_{k=1}^{N_U} c_k \hat{U}_k$. Thus, the Hamiltonian term can be evaluated through a general inner product circuit by $\langle\psi|\hat{U}_k|\phi\rangle = \langle 0|\hat{U}_\psi \hat{U}_k \hat{U}_\phi|0\rangle$ for $k = 1, \ldots, N_U$.

Specifically, the qOMM objective function

$$f(|\psi_1\rangle, \cdots, |\psi_p\rangle) = 2\sum_{i=1}^{p} \langle\psi_i|\hat{H}|\psi_i\rangle - \sum_{i,j=1}^{p} \langle\psi_i|\psi_j\rangle\langle\psi_j|\hat{H}|\psi_i\rangle, \quad \hat{H} = \sum_{k=1}^{N_U} c_k \hat{U}_k,$$

involves complex-valued terms $\langle\psi_i|\psi_j\rangle$ and $\langle\psi_i|\hat{U}_k|\psi_j\rangle$ for $i < j$, $i, j = 1, \ldots, p$, and real-valued terms $\langle\psi_i|\hat{U}_k|\psi_i\rangle$ for $i = 1, \ldots, p$. Consequently, we employ the extended Hadamard test, requiring $p^2 N_U$ inner product test circuits for the Hamiltonian part and $p(p-1)$ for the regularization part. In contrast, the objective function of qTPM and qL1M involves only real-valued terms $|\langle\psi_i|\psi_j\rangle|^2$ for $i < j$, $i, j = 1, \ldots, p$, and $\langle\psi_i|\hat{U}_k|\psi_i\rangle$ for $i = 1, \ldots, p$. Each Hamiltonian term is evaluated via a single Hadamard test and each regularization term via an inversion test, reducing the circuit counts to pN_U and $\frac{1}{2}p(p-1)$, respectively.

Table 1 summarizes the constituent terms of each objective function and the corresponding number of inner product test circuits required for their evaluation. The comparison reveals a clear trade-off: qOMM, which employs an implicit regularization, demands the highest quantum resource cost in terms of inner product test circuits. In contrast, qTPM and qL1M, utilizing explicit regularization, achieve a significant reduction in inner product test circuit overhead. This quantum resource efficiency, however, comes at the cost of increased complexity in classical optimization and hyperparameter selection. Both qTPM and qL1M introduce hyperparameters that require careful tuning, and their optimization landscapes present distinct challenges: qL1M due to its non-smooth objective function and qTPM due to its more complex local minima structure. Consequently, the selection of an appropriate model necessitates a careful balance between quantum resource constraints and classical optimization difficulty, tailored to the specific application and available hardware.

3.2. Optimization behavior. In this section, we present numerical results from noiseless, state-vector simulations for the proposed VQE models. All simulations were implemented using the Qiskit package [15]. By employing ideal quantum circuits and calculating exact probability and expectation values, we focus on the models' optimization landscapes and exclude the effects of quantum hardware noise and measurement sampling.

We apply our VQE models on the task of finding the $p = 3$ lowest eigenvalues of the electronic structure Hamiltonian within the Full Configuration Interaction (FCI)

VQE model	Hamiltonian cost		Regularization cost	
	Terms	#(Test circ)	Terms	#(Test circ)
qOMM	$\langle\psi_i|\hat{U}_k|\psi_j\rangle,\ i \leq j$	$p^2 N_U$	$\langle\psi_i|\psi_j\rangle,\ i < j$	$p(p-1)$
qTPM	$\langle\psi_i|\hat{U}_k|\psi_i\rangle$	$p N_U$	$|\langle\psi_i|\psi_j\rangle|^2,\ i < j$	$\frac{1}{2}p(p-1)$
qL1M	$\langle\psi_i|\hat{U}_k|\psi_i\rangle$	$p N_U$	$|\langle\psi_i|\psi_j\rangle|,\ i < j$	$\frac{1}{2}p(p-1)$

Table 1: Terms involved in the objective function and the number of inner product test circuits required for each VQE model. Here, N_U denotes the number of terms in the Hamiltonian decomposition, $k = 1, \ldots, N_U$ and $i, j = 1, \ldots, p$.

framework. For the molecule H_2 with a distance 0.735 Å between two hydrogen atoms, we construct the FCI Hamiltonian using PySCF [41] and map it to a qubit Hamiltonian via the Jordan-Wigner transformation. This results in a qubit Hamiltonian expressed as a linear combination of Pauli operators, which defines the Hermitian matrix A for our eigenvalue computations. All reference eigenvalues are obtained using PySCF's FCI solver.

Our numerical experiments employ the following setup for all three VQE models. We model the H_2 molecule in a minimal STO-3G basis, yielding a 4-qubit FCI Hamiltonian. The unitary coupled-cluster singles and doubles (UCCSD) ansatz is adopted for the ansatz circuit, a standard choice for quantum chemistry applications [42]. The quantum states before applying the ansatz are chosen as the Hartree-Fock state and relevant single-excitation states. The ansatz parameters are initialized to zero, which sets the UCCSD circuit to the identity operator, which naturally prepares the initial states as the Hartree-Fock state and relevant single-excitation states.

For the classical optimization, we use the derivative-free optimizers COBYLA and BOBYQA for comparison. The penalty parameters are set to $\mu = 1.0$ for qTPM and $\mu_1 = 1.0$ for qL1M, values sufficiently large to ensure the effectiveness of the regularization terms. The optimization starts with the trust region radius set to `rhobeg=1e-1` and is terminated when the trust region radius falls below a minimum value of `rhoend=1e-7` or after a maximum of 600 iterations.

To quantify convergence accuracy, we compute two relative error metrics against reference solutions. The reference objective function values f_{ref} are the theoretical values at the local minima (summarized in Table 3), and the reference eigenvalues λ_{ref} are obtained from PySCF. We measure the relative errors in the objective function and the l_2-norm of the eigenvalues, respectively, as:

$$\frac{|f_{\text{iter}} - f_{\text{ref}}|}{|f_{\text{ref}}|} \quad \text{and} \quad \frac{\|\lambda_{\text{iter}} - \lambda_{\text{ref}}\|_2}{\|\lambda_{\text{ref}}\|_2}.$$

Figure 1 displays the convergence behavior of all three models using COBYLA (left panel) and BOBYQA (right panel) optimizers, showing the relative error of the objective function versus iteration count. The corresponding accuracy of the final converged eigenvalues is quantified in Table 2 through their relative error to reference values.

For the accuracy of the final converged eigenvalues, all three models achieve chemical accuracy (`1e-3` Hartree) compared to the reference values, though qOMM and
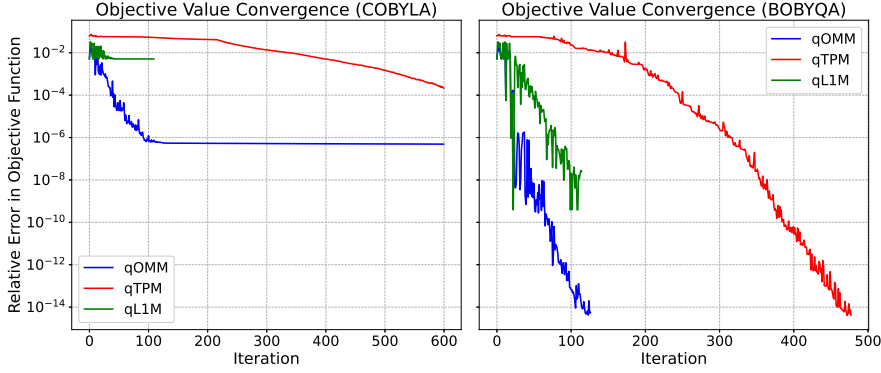
Fig. 1: Relative error of the objective function versus optimization iteration of the three VQE models for the lowest three eigenvalues of the H_2 molecule with two derivative-free optimizers: COBYLA and BOBYQA. The stop criteria is set to a minimum trust region radius of `rhoend=1e-7` or a maximum of 600 iterations.

VQE Model	Eigenstate	COBYLA	BOBYQA
qOMM	Ground	1.83×10^{-11}	5.74×10^{-15}
	1st Excited	2.25×10^{-10}	8.03×10^{-15}
	2nd Excited	1.70×10^{-8}	1.13×10^{-15}
qTPM	Ground	2.47×10^{-6}	9.56×10^{-16}
	1st Excited	2.56×10^{-6}	9.63×10^{-15}
	2nd Excited	1.09×10^{-4}	1.38×10^{-14}
qL1M	Ground	1.09×10^{-2}	8.26×10^{-10}
	1st Excited	7.31×10^{-15}	4.46×10^{-15}
	2nd Excited	1.64×10^{-15}	8.80×10^{-16}

Table 2: The relative errors of the final computed eigenvalues for each model and optimizer, compared to the reference values from PySCF.

qTPM exhibit superior precision compared to qL1M. As shown in Figure 1, qL1M is more sensitive to the choice of optimizer due to the non-smoothness of its objective function. BOBYQA yields significantly better accuracy in both the objective function value and computed eigenvalues than COBYLA. This improvement may be attributed to BOBYQA's ability to construct a quadratic model of the objective function, allowing for more informed search directions even in the presence of non-smoothness. Nevertheless, the inherent non-smoothness of qL1M remains a fundamental challenge, making optimizer selection and parameter tuning more demanding than for qOMM and qTPM when seeking comparable accuracy.

Furthermore, we note that the convergence speed varies among the three models. Specifically, qOMM demonstrates the fastest convergence in terms of number
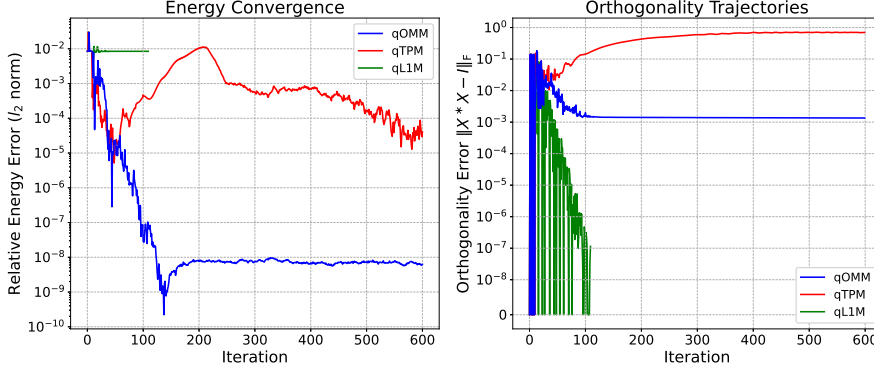
Fig. 2: Convergence of relative errors of eigenvalues and trajectories of orthogonality constraint under COBYLA optimizer for three VQE models. (Left) The convergence behavior of relative error of eigenvalues in l_2 norm for all three models. (Right) The value of $\|X^*X - I\|_{\mathrm{F}}$ versus optimization iteration for three models.

of iterations, while qTPM exhibits the slowest convergence rate. This discrepancy stems from the different landscape structures of the models. As previously discussed, qOMM's local minima directly align with the orthogonal target eigen-subspace, together with a smooth objective function, facilitating rapid convergence. In contrast, qTPM's local minima are more complex, and it requires additional refinement even after reaching the target subspace, which slows down the overall convergence. qL1M, while also targeting the orthogonal subspace, employs an l_1 penalty approach that may introduce additional complexity in the optimization landscape, resulting in a moderate convergence speed relative to the other two models.

To elucidate the connection between local minima structure and optimization behavior, we examine the convergence of orthogonality error and eigenvalue accuracy for all three VQE models using the COBYLA optimizer (Figure 2). The left panel displays the corresponding eigenvalue errors obtained via Rayleigh-Ritz at each iteration. Notably, qTPM exhibits a two-phase convergence: rapid approach to the target eigen-subspace followed by prolonged refinement toward its specific non-orthogonal minimum, requiring substantially more iterations than needed for eigenvalue estimation alone. The right panel tracks the evolution of $\|X^*X - I\|_{\mathrm{F}}$, revealing distinct orthogonality enforcement patterns: qL1M rapidly converges to zero, qOMM approaches orthogonality gradually, while qTPM converges to the theoretically predicted non-zero value of $\|\Lambda_p - \bar{\Lambda}_p\|_{\mathrm{F}} / \mu$. The patterns of orthogonality trajectories align with the convergence behaviors of the eigenvalues.

Theoretically, while all three models successfully identify the desired low-lying eigen-subspace, their distinct local minima structures (summarized in Table 3) lead to different computational behaviors. The unitary solutions of qOMM and qL1M ($X^*X = I$) reduce the Rayleigh-Ritz procedure to a standard eigenvalue problem, whereas qTPM's non-orthogonal solution ($X^*X = VSV^*$ with diagonal S and unitary V) necessitates a generalized eigenvalue problem. Furthermore, qTPM's complex minima structure impacts its convergence: even after rapidly identifying the target subspace from a good initial point, the optimization continues to refine toward its specific non-orthogonal minimum prescribed by the theory. This additional adjust-

ment, combined with the fact that optimization is terminated based solely on the objective function's convergence or a maximum iteration count, can result in a slower convergence rate for qTPM compared to qOMM and qL1M.

VQE model	Local minima form	Objective value at local minima
qOMM	$X = Q_p V^*$	$\text{tr}(\Lambda_p)$
qTPM	$X = Q_p (I - (\Lambda_p - \bar{\Lambda}_p)/\mu)^{1/2} V^*$	$\text{tr}(\Lambda_p)/2 + \text{tr}(\bar{\Lambda}_p^2 - \Lambda_p^2)/(4\mu)$
qL1M	$X = Q_p V^*$	$\text{tr}(\Lambda_p)$

Table 3: Summary of local minima for three VQE models. Here Q_p and Λ_p are eigenpairs of matrix A corresponding to the p smallest eigenvalues, $\bar{\Lambda}_p = \frac{1}{p}\text{tr}(\Lambda_p)I$, and $V \in \mathbb{C}^{p \times p}$ is unitary.

Finally, we make a comparison for the entire quantum execution time and hardware cost. The quantum resource analysis in subsection 3.1 indicates that qOMM requires approximately p times more quantum execution time per iteration than qTPM and qL1M. However, Figure 1 reveals that for $p = 3$, qOMM requires only about (or less than) $1/p$ the number of iterations to achieve a precision of `1e-14`. Consequently, the total quantum execution time of qOMM is roughly comparable to (or even less than) that of qTPM, though at the cost of greater quantum hardware resource consumption. Meanwhile, qL1M achieves reduced quantum resource requirements and execution time but demands more careful optimizer selection and tuning to attain comparable accuracy, potentially increasing classical computational overhead. These results underscore that model selection involves a trade-off between quantum resource efficiency and classical optimization complexity, which should be guided by specific application requirements and hardware constraints.

4. Conclusion. In this paper, we present the landscape analysis for three variational quantum eigensolver (VQE) models designed for excited states calculation: qOMM, qTPM, and qL1M. These models offer a solution to the challenge of enforcing orthogonality between eigenstates, by embedding the orthogonal constraint into the objective functions. These models possess the desired property that any local minimum is also a global minimum, which could be highly advantageous for optimization algorithm design. Our analysis not only provides theoretical guarantees for these favorable properties, but also offers valuable tools for landscape analysis in various other VQE models.

Among the three models proposed, qOMM uses an implicit orthogonalization approach by embedding the orthogonality constraint into the Hamiltonian term, while qTPM and qL1M employ explicit regularization terms to penalize non-orthogonality with different norms. The landscape analysis reveals distinct characteristics for each model. For qOMM and qL1M, all local minima correspond to orthogonal solutions, directly aligning with the target eigen-subspace. In contrast, qTPM's local minima are non-orthogonal but can be transformed into the desired eigen-subspace through a generalized eigenvalue problem, which increases the number of iterations. qL1M enforces orthogonality at its local minima, similar to qOMM, but utilizes an l_1-norm based penalty, leading to a non-smooth optimization landscape. This non-smoothness introduces additional complexity in the optimization process, requiring specialized algorithms to effectively navigate the landscape. The choice between these models

involves a trade-off between quantum resource demands and classical optimization complexity, with qOMM being more measurement intensive, while qTPM and qL1M offer reduced quantum costs at the expense of hyperparameter tuning and more challenging optimization.

In addition, qOMM has been previously developed into a hybrid quantum-classical algorithm with extensive numerical experiments demonstrating favorable results. For qTPM and qL1M, the current work provides an algorithmic framework with coarse-grained optimization strategies, while leaving comprehensive numerical case studies for future work. We remark that with techniques tailored to each model's particular structure, more efficient and capable algorithms may be derived to enhance applicability in the noisy intermediate-scale quantum era.

Appendix A. Proofs of qOMM.

Let us first introduce the concept of strict majorization as follows. Given a vector $x \in \mathbb{R}^n$, the notation $x^\uparrow$ denotes the reordered vector of x with entries in non-decreasing order, i.e., $x_1^\uparrow \le x_2^\uparrow \le \cdots \le x_n^\uparrow$.

DEFINITION A.1 (Strict Majorization). *Let d and λ be two vectors in $\mathbb{R}^n$. The vector λ is strictly majorized by d, if*

$$
\begin{aligned}
\lambda_1^\uparrow &< d_1^\uparrow, \\
\lambda_1^\uparrow + \lambda_2^\uparrow &< d_1^\uparrow + d_2^\uparrow,
\end{aligned}
$$

(A.1)
$$\vdots$$

$$
\begin{aligned}
\lambda_1^\uparrow + \cdots + \lambda_{n-1}^\uparrow &< d_1^\uparrow + \cdots + d_{n-1}^\uparrow, \\
\lambda_1^\uparrow + \cdots + \lambda_{n-1}^\uparrow + \lambda_n^\uparrow &= d_1^\uparrow + \cdots + d_{n-1}^\uparrow + d_n^\uparrow.
\end{aligned}
$$

LEMMA A.2. *Assume vector $\lambda \in \mathbb{R}^n$ satisfies $\lambda \ne \mathbf{1}$ and*

$$
\sum_{i=1}^n \lambda_i = \sum_{i=1}^n 1 = n,
$$

where $\mathbf{1}$ is the all-one vector in length n. Then λ is strictly majorized by $\mathbf{1}$.

Proof. Without loss of generality, we assume that λ is in non-decreasing order, i.e., $\lambda_1 \le \lambda_2 \le \cdots \le \lambda_n$. Then we can further split λ into three parts by comparing its components with 1, i.e.,

$$
\lambda_1 \le \cdots \le \lambda_i < 1 = \lambda_{i+1} = \cdots = \lambda_j < \lambda_{j+1} \le \cdots \le \lambda_n.
$$

Denote $d_1 = d_2 = \cdots = d_n = 1$. Since $\lambda \ne \mathbf{1}$, the summation condition $\sum_{i=1}^n \lambda_i = \sum_{i=1}^n d_i$ guarantees that the first and the third part are not empty. Then for the first part of λ whose values are strictly less than 1, we have

(A.2)
$$
\lambda_1 + \cdots + \lambda_k < d_1 + \cdots + d_k,
$$

for all $k = 1, \ldots, i$. For the second part, λ_is are all one. Hence, equation (A.2) is satisfied for $k = i+1, \ldots, j$. Regarding the third part, where λ_is are strictly greater than 1, if there exists an index $\ell \in \{j+1, \ldots, n-1\}$ such that

$$
\lambda_1 + \cdots + \lambda_\ell \ge d_1 + \cdots + d_\ell,
$$

then we must have $\lambda_1 + \cdots + \lambda_s > d_1 + \cdots + d_s$ for all $s > \ell$, which contradicts the summation condition $\sum_{i=1}^{n} \lambda_i = \sum_{i=1}^{n} d_i$. Combining the discussion above, we complete the proof of the lemma. $\qquad\square$

Proof of Theorem 2.1. Stationary points of (2.1) are characterized by the first-order condition of the Lagrangian function. Denoting the Lagrange multiplier by a diagonal matrix $D = \mathrm{diag}(d_1, \ldots, d_p)$, the Lagrangian function admits

$$(A.3) \qquad L(X, D) = \mathrm{tr}\left((2I - X^*X)X^*AX\right) + \mathrm{tr}(D^\top(X^*X - I)).$$

The first-order condition of (A.3) yields

$$(A.4a) \qquad \begin{cases} 2AX - AXX^*X - XX^*AX + XD = 0, \\ (A.4b) \qquad X \in \mathcal{OB}(n, p). \end{cases}$$

For any permutation matrix P, we have that (A.4) is equivalent to

$$\begin{cases} 2AXP - AXP(XP)^*XP - XP(XP)^*AXP + XPP^\top DP = 0, \\ XP \in \mathcal{OB}(n, p), \end{cases}$$

where $P^\top DP$ is a diagonal permutation of D. Therefore, without loss of generality, we assume that D has k distinct diagonal values in non-decreasing ordering,

$$D = \begin{pmatrix} d_1 I_{p_1} & & \\ & \ddots & \\ & & d_k I_{p_k} \end{pmatrix}$$

for $d_1 < d_2 < \cdots < d_k$ and p_i denoting the degeneracy of d_i. The matrix X is denoted by k column blocks, $X = (X_1, \ldots, X_k)$ following the same partition of D. The reduced singular value decomposition of each X_i admits $X_i = U_i \Sigma_i V_i^*$, where $U_i \in \mathbb{C}^{n \times r_i}, \Sigma_i \in \mathbb{R}^{r_i \times r_i}, V_i \in \mathbb{C}^{r_i \times p_i}$ for $r_i \leq p_i$ being the rank of X_i. Putting these SVDs together, we obtain the reduced SVD of X,

$$X = \begin{pmatrix} U_1 \Sigma_1 V_1^* & \cdots & U_k \Sigma_k V_k^* \end{pmatrix}$$

$$(A.5)$$

$$= \begin{pmatrix} U_1 & \cdots & U_k \end{pmatrix} \begin{pmatrix} \Sigma_1 & & \\ & \ddots & \\ & & \Sigma_k \end{pmatrix} \begin{pmatrix} V_1^* & & \\ & \ddots & \\ & & V_k^* \end{pmatrix} = U\Sigma V^*,$$

where the diagonal of Σ is not necessarily in non-increasing order.

Left multiplying X^* on both sides of (A.4a), we have

$$2X^*AX - X^*AXX^*X - X^*XX^*AX = -X^*XD,$$

whose left-hand side is Hermitian. Hence, the right-hand side X^*XD is also Hermitian, i.e., $X^*XD = DX^*X$. Substituting the block structure of X into $X^*XD = DX^*X$, we obtain,

$$(d_i - d_j)X_j^*X_i = 0, \quad i, j = 1, \ldots, k.$$

Since $d_i \neq d_j$ for $i \neq j$, we have $X_j^*X_i = 0$ and hence $U_j^*U_i = 0$.

We left multiply U^*, right multiply V, substitute the SVD of X into (A.4a), and reorganize the expression leading to

$$\text{(A.6)} \qquad \widetilde{A}\Sigma(2I - \Sigma^2) = \Sigma^2\widetilde{A}\Sigma - \Sigma D,$$

where we denote $\widetilde{A} = U^*AU$ and adopt the fact $V^*DV = D$. Recalling the block structure of X and U, we equate the left- and right-hand sides of (A.6), and obtain relations for diagonal and off-diagonal blocks,

$$\text{(A.7)} \qquad \widetilde{A}_{ii}\Sigma_i(2I - \Sigma_i^2) = \Sigma_i^2\widetilde{A}_{ii}\Sigma_i - d_i\Sigma_i, \quad i = 1,\ldots,k,$$

for diagonal blocks, and

$$\text{(A.8)} \qquad \widetilde{A}_{ij}\Sigma_j(2I - \Sigma_j^2) = \Sigma_i^2\widetilde{A}_{ij}\Sigma_j, \quad i,j = 1,\ldots,k, \text{ and } i \neq j,$$

for off-diagonal blocks, where $\widetilde{A}_{ij} = U_i^*AU_j$.

We first focus on the i-th diagonal block in (A.7). Denote the j-th diagonal entry of $\widetilde{A}_{ii}$ and Σ_i as $\tilde{a}_{ij}$ and σ_{ij}, respectively. Comparing the diagonal entries in (A.7) leads to

$$2\tilde{a}_{ij}(1 - \sigma_{ij}^2) = -d_i, \quad 1 \leq j \leq r_i.$$

By the negativity of A, we have $\tilde{a}_{ij} < 0$ for all i,j, and represent σ_{ij} by d_i and $\tilde{a}_{ij}$ as

$$\sigma_{ij}^2 = 1 + \frac{d_i}{2\tilde{a}_{ij}}.$$

Summing j from 1 to r_i, we obtain,

$$d_i = \frac{2(p_i - r_i)}{\sum_{j=1}^{r_i} \frac{1}{\tilde{a}_{ij}}},$$

where we adopt the fact that $\text{tr}(X_i^*X_i) = \sum_{j=1}^{r_i} \sigma_{ij}^2 = p_i$ by the first-order condition (A.4b). When $p_i = r_i$, i.e., X_i is of full rank, we have $d_i = 0$. Since d_i and d_j are distinct, we know that there is at most one X_i of full rank and hence at most one block such that $\sigma_{ij} = 1$. For all other strictly low-rank blocks, we have $\sigma_{ij} > 1$.

Next, we focus on the (i,j) off-diagonal block in (A.8). Comparing the (k,ℓ) elements of the (i,j) block, we have

$$\text{(A.9)} \qquad u_{ik}^*Au_{j\ell} \cdot \sigma_{j\ell}(2 - \sigma_{j\ell}^2 - \sigma_{ik}^2) = 0 \implies u_{ik}^*Au_{j\ell} = 0$$

for $k = 1,\ldots,r_i$ and $\ell = 1,\ldots,r_j$, where $u_{ik}, u_{j\ell}$ are the k-th, ℓ-th column of U_i, U_j respectively. Equation (A.9) implies the A-orthogonality of U_i and X_i, i.e.,

$$U_i^*AU_j = 0 \text{ and } X_i^*AX_j = 0,$$

for all $i \neq j$.

As we have shown that both $X_i^*X_j$ and $X_i^*AX_j$ are zero for $i \neq j$, all blocks in (A.4a) are decoupled, and satisfy

$$\text{(A.10)} \qquad 2AX_i - AX_iX_i^*X_i - X_iX_i^*AX_i + d_iX_i = 0, \quad i = 1,\ldots,k.$$

When X_i is of full-rank, we have $d_i = 0$, $\sigma_{ij} = 1$ for $j = 1, \ldots, p_i$, and X_i is a partial unitary matrix. Equation (A.10) simplifies to

$$AX_i = X_i X_i^* A X_i,$$

which implies that the column space of X_i is an invariant subspace of A. Therefore, X_i is spanned by some eigenvectors of A and such X_i satisfies the oblique manifold constraint.

Now we consider the case that X_i is strictly rank deficient. Given the basis U_i, the diagonal values of $\widetilde{A}_{ii}$ are fixed. Substituting the expression of d_i back into that of σ_{ij}^2, we have

$$\sigma_{ij} = \sqrt{1 + \frac{p_i - r_i}{\tilde{a}_{ij} \cdot \sum_{\ell=1}^{r_i} \frac{1}{\tilde{a}_{i\ell}}}} > 1.$$

To satisfy the oblique manifold constraint, i.e., $X_i \in \mathcal{OB}(n, p_i)$, we need to find a V_i such that $\operatorname{diag}(X_i^* X_i) = \mathbf{1}$. To achieve this, introduce the standard singular value decomposition of X_i from its reduced version above as

$$X_i = U_i \Sigma_i V_i^* = \begin{pmatrix} U_i & U_{i\perp} \end{pmatrix} \begin{pmatrix} \Sigma_i & 0 \\ 0 & 0 \end{pmatrix} \begin{pmatrix} V_i^* \\ V_{i\perp}^* \end{pmatrix} := \bar{U}_i \bar{\Sigma}_i \bar{V}_i^*,$$

where $\bar{U}_i \in \mathbb{C}^{n \times p_i}$, $\bar{V}_i \in \mathbb{C}^{p_i \times p_i}$. Denote $\sigma_{ij} = 0$ for $j = r_{i+1}, \ldots, p_i$, then $\sum_{j=1}^{p_i} \sigma_{ij}^2 = p_i$. By Lemma A.2, we know that $\{\sigma_{ij}^2\}_{j=1}^{p_i}$ and $\mathbf{1}$ satisfy the majorization relations. Therefore, by Schur-Horn theorem, there exists $\bar{V}_i$ unitary such that $\operatorname{diag}(\bar{V}_i \bar{\Sigma}_i^2 \bar{V}_i^*) = \mathbf{1}$, which gives the desired V_i such that $X_i \in \mathcal{OB}(n, p_i)$.

Next we analyze U_i of rank-deficient $X_i = U_i \Sigma_i V_i^*$. Denote the j-th column of U_i as u_{ij}. Comparing off-diagonal term of (A.7) we have

$$u_{ij_1}^* A u_{ij_2} (2 - \sigma_{ij_2}^2 - \sigma_{ij_1}^2) = 0, \quad j_1, j_2 = 1, \ldots, r_i, \; j_1 \neq j_2.$$

Note that $p_i > r_i$ implies $d_i < 0$ and hence $\sigma_{ij} > 1$ for $1 \leq j \leq r_i$. Therefore, $u_{ij_1}^* A u_{ij_2} = 0$ for $j_1, j_2 = 1, \ldots, r_i, j_1 \neq j_2$, which gives

$$U_i^* A U_i = \operatorname{diag}\left(\tilde{a}_{i1}, \cdots, \tilde{a}_{ir_i}\right).$$

Besides, substitute $X_i = U_i \Sigma_i V_i^*$ into (A.10), multiply $V_i \Sigma_i^{-1}$ from the right at both sides, we obtain

$$AU_i(2I - \Sigma_i^2) = U_i(\Sigma_i^2 U_i^* A U_i - d_i I).$$

Since both $U_i^* A U_i$ and $2I - \Sigma_i^2$ are diagonal, given $j = 1, \ldots, r_i$, if $\sigma_{ij}^2 \neq 2$, u_{ij} must be an eigenvector of A; if $\sigma_{ij}^2 = 2$, u_{ij} may not be the eigenvector of A.

Finally, we verify that any X satisfying the conditions in Theorem 2.1 is indeed a stationary point of qOMM. Given the combined reduced SVD form $X = U\Sigma V^*$ as in (A.5), according to conditions in Theorem 2.1,

$$U^* A U := \widetilde{A} = \operatorname{diag}(\tilde{a}_{11}, \cdots, \tilde{a}_{1r_1}, \cdots, \tilde{a}_{k1}, \cdots, \tilde{a}_{kr_k}).$$

Let

$$D = \operatorname{diag}(d_1 I_{p_1}, \cdots, d_k I_{p_k}), \quad d_i = \frac{2(p_i - r_i)}{\sum_{j=1}^{r_i} \frac{1}{\tilde{a}_{ij}}}, \; i = 1, \ldots, k.$$

Then we have $\sigma_{ij}^2 = 1 + \frac{d_i}{2\tilde{a}_{ij}}$ and $d_i = 2\tilde{a}_{ij}(\sigma_{ij}^2 - 1)$ for $j = 1, \ldots, r_i$, which gives

$$(A.11) \qquad\qquad d_i I_{r_i} = 2\widetilde{A}_i(\Sigma_i^2 - I_{r_i}),$$

where $\widetilde{A}_i = \text{diag}(\tilde{a}_{i1}, \cdots, \tilde{a}_{ir_i})$ for $i = 1, \ldots, k$. Note that for $V_i \in \mathbb{C}^{p_i \times r_i}$,

$$V_i^* d_i I_{p_i} = d_i V_i^* = d_i I_{r_i} V_i^*,$$

thus we have $V^*D = D'V^*$, where $D' = \text{diag}(d_1 I_{r_1}, \cdots, d_k I_{r_k})$. Substitute $X = U\Sigma V^*$ into the first-order condition of stationary points (A.4) we have

$$2AX - AXX^*X - XX^*AX + XD = \left(AU(2I - \Sigma^2) - U(\Sigma^2\widetilde{A} - D')\right)\Sigma V^*.$$

Note that $AU(2I - \Sigma^2) - U(\Sigma^2\widetilde{A} - D')$ can be computed block by block according to partition $U = (U_1, \cdots, U_k)$. Take one block $U_i = (u_{i1}, \cdots, u_{ir_i})$ for example, without loss of generality, we assume that $u_{i1}, \cdots, u_{i,r_i-1}$ are eigenvectors of A except u_{ir_i}. By the condition in Theorem 2.1 it leads to $\sigma_{ir_i}^2 = 2$. Therefore,

$$AU_i(2I - \Sigma_i^2)$$

$$= (u_{i1}, \cdots, u_{i,r_i-1}, Au_{ir_i}) \begin{pmatrix} \tilde{a}_{i1} & & & \\ & \ddots & & \\ & & \tilde{a}_{i,r_i-1} & \\ & & & 1 \end{pmatrix} \begin{pmatrix} 2 - \sigma_{i1}^2 & & & \\ & \ddots & & \\ & & 2 - \sigma_{i,r_i-1}^2 & \\ & & & 0 \end{pmatrix}$$

$$= (u_{i1}, \cdots, u_{i,r_i-1}, u_{ir_i}) \begin{pmatrix} \tilde{a}_{i1} & & & \\ & \ddots & & \\ & & \tilde{a}_{i,r_i-1} & \\ & & & \tilde{a}_{ir_i} \end{pmatrix} \begin{pmatrix} 2 - \sigma_{i1}^2 & & & \\ & \ddots & & \\ & & 2 - \sigma_{i,r_i-1}^2 & \\ & & & 0 \end{pmatrix}$$

$$= U_i\widetilde{A}_i(2I - \Sigma_i^2).$$

Thus, according to (A.11) we have

$$AU_i(2I - \Sigma_i^2) - U_i(\Sigma_i^2\widetilde{A}_i - d_i I_{r_i}) = U_i\left(\widetilde{A}_i(2I - \Sigma_i^2) - \Sigma_i^2\widetilde{A}_i + d_i I_{r_i}\right) = 0,$$

which implies that

$$2AX - AXX^*X - XX^*AX + XD = \left(AU(2I - \Sigma^2) - U(\Sigma^2\widetilde{A} - D')\right)\Sigma V^* = 0.$$

Therefore, such X is a stationary point of qOMM. $\qquad\qquad\qquad\qquad\square$

To further distinguish the local minimizers from stationary points, we introduce the concept of strong Schur-Horn continuity, which plays a key role during the construction of descent direction near the stationary point that is not a local minimizer.

DEFINITION A.3 (Strong Schur-Horn Continuity [7]). *Suppose $A \in \mathbb{C}^{n \times n}$ is a Hermitian matrix with an eigendecomposition $A = Q\Lambda Q^*$, where Q is the unitary eigenvector matrix and Λ is the diagonal eigenvalue matrix. Matrix A is strongly Schur-Horn continuous if, for any perturbed eigenvalues $\widetilde{\Lambda}$ satisfying $\text{tr}(\widetilde{\Lambda}) = \text{tr}(\Lambda)$ and $\left\|\widetilde{\Lambda} - \Lambda\right\|_F = O(\varepsilon)$ for $\varepsilon > 0$ sufficiently small, there exists a Hermitian matrix $\widetilde{B} = G_2 Q G_1 \widetilde{\Lambda} G_1^* Q^* G_2^*$ such that*

1. $\operatorname{diag}(\widetilde{B}) = \operatorname{diag}(A)$,
2. G_1 and G_2 are unitary matrices, and
3. $\|G_i - I\|_{\mathrm{F}} = O(\varepsilon^{1/2})$ for $i = 1, 2$.

Furthermore, we have the following proposition for strong Schur-Horn continuity.

PROPOSITION A.4 ([7]). *If $A \in \mathbb{C}^{n \times n}$ is a Hermitian matrix whose eigenvalue is strictly majorized by the diagonal, then A is strongly Schur-Horn continuous.*

Lemma A.5 essentially applies the strong Schur-Horn continuity to singular values of a matrix, and obtains a construction for perturbed singular value decomposition of a point in oblique manifold.

LEMMA A.5. *Suppose $X \in \mathcal{OB}(n, p)$ is non-unitary with a singular value decomposition $X = U\Sigma V^*$, where $U \in \mathbb{C}^{n \times p}$, $\Sigma \in \mathbb{R}^{p \times p}$ whose diagonal entries may not be in a non-increasing order and $V \in \mathbb{C}^{p \times p}$. Given any perturbed singular values $\widetilde{\Sigma} \in \mathbb{R}^{p \times p}$ such that*

$$\operatorname{tr}(\widetilde{\Sigma}^2) = \operatorname{tr}(\Sigma^2) \quad and \quad \left\|\widetilde{\Sigma}^2 - \Sigma^2\right\|_{\mathrm{F}} = O(\varepsilon),$$

for $\varepsilon > 0$ sufficiently small, there exist unitary $\widetilde{V} \in \mathbb{C}^{p \times p}$ such that $\widetilde{X} := U\widetilde{\Sigma}\widetilde{V}^* \in \mathcal{OB}(n, p)$ and

$$\left\|\widetilde{X} - X\right\|_{\mathrm{F}} = O(\varepsilon^{1/2}).$$

Proof. Denote $H := X^*X = V\Sigma^2 V^*$ and $s := \operatorname{diag}(\Sigma^2)$. Since X is a point on oblique manifold, we have $\sum_{i=1}^p s_i = \operatorname{tr}(H) = p$ and $\operatorname{diag}(H) = \mathbf{1}$. According to Lemma A.2, s is strictly majorized by $\mathbf{1}$. Therefore, Proposition A.4 implies that H is strongly Schur-Horn continuous, and there exists

$$\widetilde{H} = G_2 V G_1 \widetilde{\Sigma}^2 G_1^* V^* G_2^*$$

such that $\operatorname{diag}(\widetilde{H}) = \operatorname{diag}(H) = \mathbf{1}$, G_i is unitary, and $\|G_i - I\|_{\mathrm{F}} = O(\varepsilon^{1/2})$ for $i = 1, 2$. Let $\widetilde{V} = G_2 V G_1$. Then, the distance between V and $\widetilde{V}$ is bounded by

$$\left\|\widetilde{V} - V\right\|_{\mathrm{F}} = \|G_2 V G_1 - G_2 V + G_2 V - V\|_{\mathrm{F}} \leq \|G_1 - I\|_{\mathrm{F}} + \|G_2 - I\|_{\mathrm{F}} = O(\varepsilon^{1/2}),$$

where we use the unitary invariance of Frobenius norm. Constructing the perturbed $\widetilde{X}$ as $\widetilde{X} = U\widetilde{\Sigma}\widetilde{V}^*$, we know that $\widetilde{X} \in \mathcal{OB}(n, p)$ following $\operatorname{diag}(\widetilde{X}^*\widetilde{X}) = \operatorname{diag}(\widetilde{H}) = \mathbf{1}$. Furthermore, the distance between X and $\widetilde{X}$ could be bounded as,

$$\left\|\widetilde{X} - X\right\|_{\mathrm{F}} = \left\|U\widetilde{\Sigma}\widetilde{V}^* - U\Sigma V^*\right\|_{\mathrm{F}} \leq \left\|\widetilde{\Sigma} - \Sigma\right\|_{\mathrm{F}} + \|\Sigma\|_{\mathrm{F}} \left\|\widetilde{V}^* - V^*\right\|_{\mathrm{F}} = O(\varepsilon^{1/2}),$$

which completes the proof. $\square$

Proof of Theorem 2.3. Given the combined reduced SVD of any stationary point $X = U\Sigma V^*$ as in (A.5), one can always expand the SVD to include zero singular values, i.e.,

$$X_i = U_i \Sigma_i V_i^* = \begin{pmatrix} U_i & U_{i\perp} \end{pmatrix} \begin{pmatrix} \Sigma_i & 0 \\ 0 & 0 \end{pmatrix} \begin{pmatrix} V_i^* \\ V_{i\perp}^* \end{pmatrix} =: \bar{U}_i \bar{\Sigma}_i \bar{V}_i^*,$$

where $\bar{U}_i \in \mathbb{C}^{n \times p_i}$ is a partial unitary matrix, $\bar{\Sigma}_i \in \mathbb{R}^{p_i \times p_i}$ is a diagonal matrix, $\bar{V}_i \in \mathbb{C}^{p_i \times p_i}$ is a unitary matrix, and $\bar{U}_i^* \bar{U}_j = 0$ for all $1 \leq i \neq j \leq k$. Combining these

SVDs similarly to that in (A.5), we obtain,

$$X = \begin{pmatrix} \bar{U}_1\bar{\Sigma}_1\bar{V}_1^* & \cdots & \bar{U}_k\bar{\Sigma}_k\bar{V}_k^* \end{pmatrix}$$

$$= \begin{pmatrix} \bar{U}_1 & \cdots & \bar{U}_k \end{pmatrix} \begin{pmatrix} \bar{\Sigma}_1 & & \\ & \ddots & \\ & & \bar{\Sigma}_k \end{pmatrix} \begin{pmatrix} \bar{V}_1^* & & \\ & \ddots & \\ & & \bar{V}_k^* \end{pmatrix} = \bar{U}\bar{\Sigma}\bar{V}^*.$$

Denoting the j-th diagonal entries of $\bar{U}_i^* A \bar{U}_i$ as $\tilde{a}_{ij}$ for $j = 1, \ldots, p_i$ and $i = 1, \ldots, k$, the objective value at $X = \bar{U}\bar{\Sigma}\bar{V}^*$ admits,

$$E_0(X) = \sum_{i=1}^{k} \text{tr}\left((2I - \bar{\Sigma}_i^2)\bar{\Sigma}_i\bar{U}_i^* A \bar{U}_i \bar{\Sigma}_i\right) = \sum_{i=1}^{k}\sum_{j=1}^{r_i} \tilde{a}_{ij}(2 - \sigma_{ij}^2)\sigma_{ij}^2.$$

Notice that $\tilde{a}_{ij}$s are all negative since A is negative definite. In the following, we give the decay direction for low-rank X and full-rank X, respectively.

First, we consider stationary points X that are of strict low-rank. In arbitrary ε-neighborhood of X for $\varepsilon > 0$ sufficiently small, we construct a perturbed point $\widetilde{X} = \bar{U}\widetilde{\Sigma}\widetilde{V}^*$ such that

$$\widetilde{\Sigma}^2 = (1 - \varepsilon)\Sigma^2 + \varepsilon I.$$

One has $\text{tr}(\widetilde{\Sigma}^2) = \text{tr}(\Sigma^2)$ and $\left\|\widetilde{\Sigma}^2 - \Sigma^2\right\|_{\text{F}} = O(\varepsilon)$. According to Lemma A.5, there exists $\widetilde{V} \in \mathbb{C}^{p \times p}$ such that $\widetilde{X} = \bar{U}\widetilde{\Sigma}\widetilde{V}^* \in \mathcal{OB}(n, p)$ and $\left\|\widetilde{X} - X\right\|_{\text{F}} = O(\varepsilon^{1/2})$. The difference between the objective values at $\widetilde{X}$ and X is bounded as,

$$E_0(\widetilde{X}) - E_0(X) = \sum_{i=1}^{k}\sum_{j=1}^{r_i} \tilde{a}_{ij}(2 - \varepsilon)\varepsilon(\sigma_{ij}^2 - 1)^2 + \sum_{i=1}^{k}\sum_{j=r_i+1}^{p_i} \tilde{a}_{ij}(2 - \varepsilon)\varepsilon < 0.$$

Thus, for sufficiently small $\varepsilon > 0$, there exists $\widetilde{X} \in \mathcal{OB}(n, p)$ such that $\left\|\widetilde{X} - X\right\|_{\text{F}} = O(\varepsilon^{1/2})$ and $E_0(\widetilde{X}) < E_0(X)$. The rank-deficient stationary points are strict saddle points.

Next, we consider the full rank stationary point X. According to Theorem 2.1, full rank stationary point is of form $X = UV^*$, with $U \in \mathbb{C}^{n \times p}$ being orthonormal eigenvectors of A and $V \in \mathbb{C}^{p \times p}$ is unitary. Denote the unitary eigenvector matrix of A as $Q = \begin{pmatrix} q_1 & \cdots & q_n \end{pmatrix}$, whose corresponding eigenvalues are $\lambda_1 \leq \cdots \leq \lambda_n$. If U is not spanned by eigenvectors corresponding to the p smallest eigenvalues, then there exist a column in U, denote as u_s, with eigenvalue $\tilde{\lambda} > \lambda_p$, and another $q_t \notin \text{span}(U)$ with $t \leq p$ and $\lambda_t \leq \lambda_p < \tilde{\lambda}$. We construct a perturbed point as

$$\widetilde{X} = \widetilde{U}V^* = \begin{pmatrix} u_1 & \cdots & u_{s-1} & \sqrt{1 - \varepsilon^2}u_s + \varepsilon q_t & u_{s+1} & \cdots & u_p \end{pmatrix} V^*.$$

We could verify that $\widetilde{X} \in \mathcal{OB}(n, p)$ and $\left\|\widetilde{X} - X\right\|_{\text{F}} = O(\varepsilon)$. The difference between objective values at $\widetilde{X}$ and X is bounded as,

$$E_0(\widetilde{X}) - E_0(X) = \varepsilon^2(\lambda_t - \tilde{\lambda}) < 0.$$

Thus, if U is not spanned by eigenvectors corresponding to the p smallest eigenvalues, X is not a local minimizer.

We have previously demonstrated that any local minimizer of qOMM takes the form $X = Q_pV^*$, where Q_p are eigenvectors of A corresponding to the p smallest eigenvalues Λ_p and $V \in \mathbb{C}^{p \times p}$ unitary. Substituting $X = Q_pV^*$ into the energy functional $E_0(X)$ it yields the same objective value $E_0(Q_pV^*) = \text{tr}(\Lambda_p)$. Hence, any local minimum of qOMM is also a global minimum.

Finally, note that oblique manifold $\mathcal{OB}(n, p)$ is a bounded and closed set and the objective function $E_0(X)$ is smooth with respect to X, there exists a minimum of $E_0(X)$ over $\mathcal{OB}(n, p)$. Thus, we conclude that any matrix in the form $X = Q_pV^*$ is a global minimizer of qOMM and there is no other local minimizer. $\qquad\square$

Appendix B. Proofs of qTPM.

The proofs of theorems of qTPM follow a similar procedure as qOMM above, hence we present the main steps and emphasize the differences owing to the nature of qTPM. Some detailed derivation may not appear again for simplicity.

Proof of Theorem 2.6. The Lagrangian multiplier function of qTPM is

$$
\begin{aligned}
L(X, D) :=& g_\mu(X) + \frac{1}{2}\sum_{i=1}^{p} d_i(x_i^* x_i - 1) \\
=& \frac{1}{2}\text{tr}(X^*AX) + \frac{\mu}{4}\text{tr}(X^*XX^*X) + \frac{1}{2}\text{tr}(D^\top(X^*X - I)),
\end{aligned}
$$

then the first-order condition of stationary points gives

$$
\begin{cases}
AX + \mu XX^*X + XD = 0, \\
X \in \mathcal{OB}(n, p).
\end{cases}
$$

(B.1a)

(B.1b)

Note that $g_\mu(X)$ is invariant under right multiplication of permutation matrices. Similar to the proof of Theorem 2.1, without loss of generality, we assume

$$
D = \text{diag}\left(d_1 I_{p_1}, \cdots, d_k I_{p_k}\right),
$$

with $d_1 < d_2 < \cdots < d_k$ and $p_1 + \cdots + p_k = p$. Correspondingly, we divide the columns of X into k parts $X = (X_1, \cdots, X_k)$ in the same way as D. Applying singular value decomposition to each block of X one has $X_i = U_i\Sigma_i V_i^*$ where $U_i \in \mathbb{C}^{n \times p_i}, \Sigma_i \in \mathbb{R}^{p_i \times p_i}$ and $V_i \in \mathbb{C}^{p_i \times p_i}$ for $i = 1, \ldots, k$. Thus,

$$
X = \begin{pmatrix} U_1 & \cdots & U_k \end{pmatrix} \begin{pmatrix} \Sigma_1 & & \\ & \ddots & \\ & & \Sigma_k \end{pmatrix} \begin{pmatrix} V_1^* & & \\ & \ddots & \\ & & V_k^* \end{pmatrix} := U\Sigma V^*.
$$

Multiplying X^* from the left at both sides of (B.1a) we have

$$
X^*AX + \mu X^*XX^*X + X^*XD = 0,
$$

which implies that $X^*XD = DX^*X$ and further, $(d_i - d_j)X_j^*X_i = 0$ for $i, j = 1, \ldots, k$. Thus, we have $X_j^*X_i = 0$ for $i \neq j$. Substitute the block partition of X and D into (B.1a), utilizing $X_j^*X_i = 0$ for $i \neq j$ it yields

$$
AX_i + \mu X_i X_i^* X_i + d_i X_i = 0, \quad i = 1, \ldots, k.
$$

(B.2)

Substitute $X_i = U_i\Sigma_i V_i^*$ into (B.2) for each block, multiplying U_i^* from the left and multiplying V_i from the right we arrive at

$$
\widetilde{A}_i \Sigma_i + \mu \Sigma_i^3 = -d_i\Sigma_i, \quad i = 1, \ldots, k,
$$

(B.3)

where we denote $\widetilde{A}_i = U_i^* A U_i$.

To determine U, denote the j-th column of U_i as u_{ij}, comparing off-diagonal terms of (B.3) we have

$$u_{ij_1}^* A u_{ij_2} \sigma_{ij_2} = 0, \quad j_1, j_2 = 1, \ldots, r_i, \; j_1 \neq j_2.$$

Denote $\text{rank}(X_i) = r_i$ for $i = 1, \ldots, k$. Since $\sigma_{ij} > 0$ for $1 \leq j \leq r_i$, $u_{ij_1}^* A u_{ij_2} = 0$ for $j_1, j_2 = 1, \ldots, r_i, j_1 \neq j_2$. Denote the corresponding reduced singular value decomposition of X_i as

$$X_i = U_i \Sigma_i V_i^* = \begin{pmatrix} U_{i1} & U_{i2} \end{pmatrix} \begin{pmatrix} \Sigma_{i1} & 0 \\ 0 & 0 \end{pmatrix} \begin{pmatrix} V_{i1}^* \\ V_{i2}^* \end{pmatrix} = U_{i1} \Sigma_{i1} V_{i1}^*.$$

Then we know that $U_{i1}^* A U_{i1}$ is diagonal. Furthermore, since X_i and U_{i1} are invariant subspaces of matrix A by (B.2), U_{i1} consists of mutually orthogonal eigenvectors of A. Besides, from $X_i^* X_j = 0$ for $i \neq j$, we have $U_{i1}^* U_{j1} = 0$. Thus, in order to give a compact form of X, we choose U_{i2} corresponding to zero singular values for $i = 1, \ldots, k$ to be eigenvectors of A such that $U = (U_1, \cdots, U_k)$ is unitary, i.e., $U^* U = I$.

Next we figure out the singular values of X_i for $i = 1, \cdots, k$. Denote the diagonal entries of $U_i^* A U_i$ as λ_{ij} for $j = 1, \ldots, p_i$. Comparing diagonal terms of (B.3) we have

$$\lambda_{ij} \sigma_{ij} + \mu \sigma_{ij}^3 = -d_i \sigma_{ij}, \quad j = 1, \ldots, p_i.$$

Since A is negative definite, $\lambda_{ij} < 0$. Note that $\sigma_{ij} > 0$ for $1 \leq j \leq r_i$, we have

$$\sigma_{ij}^2 = -\frac{\lambda_{ij} + d_i}{\mu}, \quad j = 1, \ldots, r_i.$$

Summing up j from 1 to r_i we obtain,

$$d_i = -\frac{1}{r_i} \Big(\sum_{j=1}^{r_i} \lambda_{ij} + \mu p_i \Big),$$

where we adopt the fact that $\text{tr}(X_i^* X_i) = \sum_{j=1}^{r_i} \sigma_{ij}^2 = p_i$ by the first-order condition (B.1b). Therefore, we get

$$\sigma_{ij}^2 = \frac{p_i}{r_i} - \frac{1}{\mu}(\lambda_{ij} - \frac{1}{r_i} \sum_{l=1}^{r_i} \lambda_{il}) := \frac{p_i}{r_i} - \frac{1}{\mu} \left(\lambda_{ij} - \bar{\lambda}_i \right), \quad j = 1, \ldots, r_i.$$

Now we check the consistency for stationary points satisfying the first-order condition (B.1). Note that A is negative definite and $\mu > |\lambda_{\min}(A)|$, we have

$$\mu > -\lambda_{\min}(A) \geq -\bar{\lambda}_i \geq \frac{r_i}{p_i}(\lambda_{ij} - \bar{\lambda}_i), \quad j = 1, \ldots, r_i, i = 1, \ldots, k,$$

which ensures that $\sigma_{ij}^2 > 0$ for $j = 1, \ldots, r_i$ and $i = 1, \ldots, k$. Given $i = 1, \ldots, k$, if σ_{ij}^2 are not all ones for $j = 1, \ldots, p_i$, according to Lemma A.2, $\{\sigma_{ij}\}_{j=1}^{p_i}$ and $\mathbf{1}$ satisfy the majorization relation. Thus, by Schur-Horn theorem, there exists $V_i \in \mathbb{C}^{p_i \times p_i}$ unitary such that $\text{diag}(V_i \Sigma_i^2 V_i^*) = \mathbf{1}$. Hence, we conclude that there always exists unitary V_i such that $X_i = U_i \Sigma_i V_i$ satisfies the oblique manifold constraint.

Finally, we verify that any X satisfying the conditions in Theorem 2.6 is indeed a stationary point of qTPM, i.e., there exists a diagonal matrix D such that

$$AX + \mu X X^* X + X D = 0.$$

Given the singular value decomposition $X = U\Sigma V^*$ as in Theorem 2.6, let

$$D = \text{diag}(d_1 I_{p_1}, \cdots, d_k I_{p_k}), \quad d_i = -\frac{1}{r_i}\left(\mu p_i + \sum_{j=1}^{r_i} \lambda_{ij}\right), \ i = 1, \ldots, k.$$

Then we have $V^*D = DV^*$. Since $AU = U\Lambda$, where

$$\Lambda = \text{diag}\left(\lambda_{11}, \cdots, \lambda_{1p_1}, \cdots, \lambda_{k1}, \cdots, \lambda_{kp_k}\right),$$

it yields

$$AX + \mu XX^*X + XD = U\Sigma\left(\Lambda + \mu\Sigma^2 + D\right)V^*.$$

From the expression of Σ in Theorem 2.6, one can easily see that $\Sigma\left(\Lambda + \mu\Sigma^2 + D\right) = 0$ and hence $AX + \mu XX^*X + XD = 0$. Therefore, such X is a stationary point of qTPM. $\qquad\qquad\qquad\qquad\qquad\qquad\qquad\qquad\qquad\qquad\qquad\qquad\qquad\qquad\square$

Proof of Theorem 2.7. According to Theorem 2.6, stationary points of qTPM (2.4) take the form $X = U\Sigma V^*$ with $U^*U = I_p$ and $V^*V = I_p$. Besides, $U^*AU = \Lambda$ is diagonal with eigenvalues $\lambda_{11}, \cdots, \lambda_{1p_1}, \cdots, \lambda_{k1}, \cdots, \lambda_{kp_k}$ of A being its diagonal entries. Then we can rewrite the objective value of qTPM at stationary point X as

$$g_\mu(X) = \frac{1}{2}\text{tr}(V\Sigma U^*AU\Sigma V^*) + \frac{\mu}{4}\text{tr}(V\Sigma U^*U\Sigma V^*V\Sigma U^*U\Sigma V^*)$$

$$= \frac{1}{2}\text{tr}(\Lambda\Sigma^2) + \frac{\mu}{4}\text{tr}(\Sigma^4) = \frac{1}{2}\sum_{i=1}^{k}\sum_{j=1}^{p_i}(\lambda_{ij} + \frac{\mu}{2}\sigma_{ij}^2)\sigma_{ij}^2.$$

Thus, the objective value at stationary points relies on the eigenvalues and singular values. In the following, we construct descent directions for stationary points that are strictly saddle points.

First, we show that any rank deficient stationary point is a strict saddle point. Given the singular value decomposition of $X = U\Sigma V^*$ as in Theorem 2.6, if X is rank deficient, there exists at least a block of Σ, denoted as Σ_i, such that $r_i < p_i$. The diagonal entries of Σ_i are

$$\sigma_{ij} = \sqrt{\frac{p_i}{r_i} - \frac{1}{\mu}\left(\lambda_{ij} - \bar{\lambda}_i\right)}, \quad j = 1, \ldots, r_i; \quad \sigma_{ij} = 0, \quad j = r_{i+1}, \ldots, p_i,$$

where we denote $\bar{\lambda}_i = \frac{1}{r_i}\sum_{l=1}^{r_i}\lambda_{il}$. Given $\varepsilon > 0$ sufficiently small, consider the perturbation $\widetilde{\Sigma}$ of singular values Σ by introducing

$$\tilde{\sigma}_{i1}^2 = \sigma_{i1}^2 - \varepsilon, \quad \tilde{\sigma}_{ip_i}^2 = \sigma_{ip_i}^2 + \varepsilon = \varepsilon,$$

where we adopt the fact that $\sigma_{ip_i} = 0$. All the other entries in $\widetilde{\Sigma}$ are the same as Σ. Then we have $\text{tr}(\widetilde{\Sigma}^2) = \text{tr}(\Sigma^2)$ and $\left\|\widetilde{\Sigma}^2 - \Sigma^2\right\|_{\text{F}} = O(\varepsilon)$. According to Lemma A.5, there exists $\widetilde{V} \in \mathbb{C}^{n \times n}$ such that $\widetilde{X} = U\widetilde{\Sigma}\widetilde{V}^* \in \mathcal{OB}(n, p)$ and $\left\|\widetilde{X} - X\right\|_{\text{F}} = O(\varepsilon^{1/2})$. Thus, $\widetilde{X}$ is a perturbation of X over oblique manifold with desired singular values.

At this time, we have

$$g_\mu(\widetilde{X}) - g_\mu(X) = \frac{1}{2}(\lambda_{i1} + \frac{\mu}{2}\tilde{\sigma}_{i1}^2)\tilde{\sigma}_{i1}^2 - \frac{1}{2}(\lambda_{i1} + \frac{\mu}{2}\sigma_{i1}^2)\sigma_{i1}^2 + \frac{1}{2}(\lambda_{ip_i} + \frac{\mu}{2}\tilde{\sigma}_{ip_i}^2)\tilde{\sigma}_{ip_i}^2$$

$$= \frac{1}{2}\left(\lambda_{ip_i} - (\bar{\lambda}_i + \frac{p_i}{r_i}\mu)\right)\varepsilon + \frac{1}{2}\mu\varepsilon^2.$$

Note that $\lambda_{ip_i} < 0$ since A is negative definite. Besides,

$$\bar{\lambda}_i + \frac{p_i}{r_i}\mu > \bar{\lambda}_i + \mu > \bar{\lambda}_i + |\lambda_{\min}(A)| \geq 0.$$

Therefore, $g_\mu(\widetilde{X}) - g_\mu(X) < 0$ when $\varepsilon > 0$ is sufficiently small. Such rank deficient stationary point has a descent direction and is a strict saddle point.

Next we turn to the full rank stationary points $X = U\Sigma V^*$. According to Theorem 2.6, the singular value matrix Σ of full rank X satisfies

$$\Sigma^2 = I - \frac{1}{\mu}\begin{pmatrix} \Lambda_1 & & \\ & \ddots & \\ & & \Lambda_k \end{pmatrix} + \frac{1}{\mu}\begin{pmatrix} \bar{\lambda}_1 I_{p_1} & & \\ & \ddots & \\ & & \bar{\lambda}_k I_{p_k} \end{pmatrix},$$

where we denote the average value $\bar{\lambda}_i = \frac{1}{p_i}\sum_{j=1}^{p_i}\lambda_{ij}$ for $i = 1, \ldots, k$. Note that those blocks with the same average value can be merged through a permutation. Without loss of generality, we assume $\bar{\lambda}_i \neq \bar{\lambda}_j$ for $i, j \in \{1, \ldots, k\}, i \neq j$. Now we show that any singular value matrix Σ with $k > 1$ is a strict saddle point. Assume that X is a full rank stationary point with $k > 1$, then one can always find two blocks with indices i and j such that $\bar{\lambda}_i < \bar{\lambda}_j$. Given $\varepsilon > 0$ sufficiently small, consider a perturbation $\widetilde{\Sigma}$ of original Σ by introducing

$$\tilde{\sigma}_{i1}^2 = \sigma_{i1}^2 + \varepsilon, \quad \tilde{\sigma}_{j1}^2 = \sigma_{j1}^2 - \varepsilon,$$

while keeping all the other singular values in $\widetilde{\Sigma}$ the same as Σ. Then we have $\text{tr}(\widetilde{\Sigma}^2) = \text{tr}(\Sigma^2)$ and $\left\|\widetilde{\Sigma}^2 - \Sigma^2\right\|_F = O(\varepsilon)$. According to Lemma A.5, there exists $\widetilde{V} \in \mathbb{C}^{n \times n}$ such that $\widetilde{X} = U\widetilde{\Sigma}\widetilde{V}^* \in \mathcal{OB}(n, p)$ and $\left\|\widetilde{X} - X\right\|_F = O(\varepsilon^{1/2})$. Thus, $\widetilde{X}$ is a perturbation of X over oblique manifold with desired singular values. At this time, we have

$$g_\mu(\widetilde{X}) - g_\mu(X)$$
$$= \frac{1}{2}(\lambda_{i1} + \frac{\mu}{2}\tilde{\sigma}_{i1}^2)\tilde{\sigma}_{i1}^2 - \frac{1}{2}(\lambda_{i1} + \frac{\mu}{2}\sigma_{i1}^2)\sigma_{i1}^2 + \frac{1}{2}(\lambda_{j1} + \frac{\mu}{2}\tilde{\sigma}_{j1}^2)\tilde{\sigma}_{j1}^2 - \frac{1}{2}(\lambda_{j1} + \frac{\mu}{2}\sigma_{j1}^2)\sigma_{j1}^2$$
$$= \frac{1}{2}(\bar{\lambda}_i - \bar{\lambda}_j)\varepsilon + \frac{1}{2}\mu\varepsilon^2 < 0,$$

when $\varepsilon > 0$ is sufficiently small. Thus, those full rank stationary points X with $k > 1$ are all strict saddle points.

Finally, we consider the selection of eigenvectors. We have shown that any local minimizer has a singular value decomposition $X = U\Sigma V^*$ where U consists of eigenvectors of matrix A, $V \in \mathbb{C}^{n \times n}$ unitary such that $\text{diag}(X^*X) = \mathbf{1}$. Denote the ordered eigenvectors of A as $\begin{pmatrix} q_1 & \cdots & q_n \end{pmatrix}$ with corresponding eigenvalues $\lambda_1 \leq \cdots \leq \lambda_n$. If U is not spanned by eigenvectors corresponding to the p most smallest eigenvalues, then there exists a column in U, denoted as u_s, with eigenvalue $\tilde{\lambda} > \lambda_p$, and another

$q_t \notin \text{span}(U)$ with $t \leq p$ and $\lambda_t \leq \lambda_p < \tilde{\lambda}$. We construct a perturbed point as

$$\widetilde{X} = \widetilde{U}\Sigma V^* = \begin{pmatrix} u_1 & \cdots & u_{s-1} & \sqrt{1-\varepsilon^2}u_s + \varepsilon q_t & u_{s+1} & \cdots & u_p \end{pmatrix} \Sigma V^*.$$

One could verify that $\widetilde{X} \in \mathcal{OB}(n,p)$ and $\left\|\widetilde{X} - X\right\|_{\text{F}} = O(\varepsilon)$. The difference between objective values at $\widetilde{X}$ and X is bounded as,

$$g_\mu(\widetilde{X}) - g_\mu(X) = \frac{1}{2}\varepsilon^2(\lambda_p - \tilde{\lambda})\sigma_s^2 < 0.$$

Thus, if U is not spanned by eigenvectors corresponding to the p smallest eigenvalues, X is not a local minimizer.

Therefore, any local minimizer of qTPM takes the form $X = Q_p(I - \frac{1}{\mu}(\Lambda_p - \bar{\Lambda}_p))^{1/2}V^*$, where Q_p and Λ_p are eigenpairs of A corresponding to the p smallest eigenvalues, $\bar{\Lambda}_p = \frac{1}{p}\text{tr}(\Lambda_p)I$. Substituting $X = Q_p(I - \frac{1}{\mu}(\Lambda_p - \bar{\Lambda}_p))^{1/2}V^*$ into the energy functional $g_\mu(X)$ yields the same objective value

$$g_\mu\left(Q_p(I - \frac{1}{\mu}(\Lambda_p - \bar{\Lambda}_p))^{1/2}V^*\right) = \frac{\mu}{4}\text{tr}\left((I + \frac{1}{\mu}\bar{\Lambda}_p)^2 - \frac{1}{\mu^2}\Lambda_p^2\right).$$

Again, since oblique manifold $\mathcal{OB}(n,p)$ is a bounded and closed set and the objective function $g_\mu(X)$ is smooth with respect to X, there exists a global minimum of $g_\mu(X)$ over $\mathcal{OB}(n,p)$. Thus, we conclude that any matrix in the form $X = Q_p(I - \frac{1}{\mu}(\Lambda_p - \bar{\Lambda}_p))^{1/2}V^*$ is a global minimizer of qTPM and there is no other local minimizer. □

Appendix C. Proofs of qL1M.

LEMMA C.1. *Given matrix $X = (x_1, \cdots, x_p) \in \mathbb{C}^{n \times p}$ and vector $x_0 \in \mathbb{C}^{n \times 1}$ such that $x_0 \notin span(X)$, there exists $d \in \mathbb{C}^{n \times 1}$ such that*

$$d^*d = 1, \quad d^*X = 0, \quad d^*x_0 < 0.$$

Additionally, if for $i, j = 0, 1, \cdots, p$, $i \neq j$,

(C.1) $$x_i^*x_i = 1, \quad |x_i^*x_j| \leq \varepsilon_0,$$

where $\varepsilon_0 = \frac{1}{4p}$, then there exists $d \in \mathbb{C}^{n \times 1}$ such that

$$d^*d = 1, \quad d^*X = 0, \quad d^*x_0 < -\frac{1}{2}.$$

Proof. Denote the orthogonal projection of x_0 over $span(X)$ as $s = XX^\dagger x_0$. Since $x_0 \notin span(X)$, let

$$d = \frac{s - x_0}{\|s - x_0\|_2},$$

then we have

$$d^*d = 1, \quad d^*X = 0, \quad d^*x_0 = d^*(s - \|s - x_0\|_2\, d) = -\|s - x_0\|_2 < 0,$$

which completes the proof of the first statement.

Next we give a lower bound of $\|s - x_0\|_2$ based on condition (C.1). According to Gerschgorin disk theorem, eigenvalues of X^*X lie in disks

$$G_i = \left\{ z \in \mathbb{C} : |z - 1| \leq \sum_{j \neq i}^{p} |(X^*X)_{ij}| \leq p\varepsilon_0 < \frac{1}{2} \right\}, \quad i = 1, \cdots, p.$$

Thus, X^*X is non-singular and all the eigenvalues of X^*X lie in $[\frac{1}{2}, \frac{3}{2}]$. Moreover, all the eigenvalues of $(X^*X)^{-1}$ lie in $[\frac{2}{3}, 2]$. Therefore,

$$\|X\|_2 \leq \sqrt{\frac{3}{2}}, \quad \|(X^*X)^{-1}\|_2 \leq 2.$$

Note that $|(X^*x_0)_j| = |x_j^*x_0| \leq \varepsilon_0$ for $j = 1, \ldots, p$. At this time, we have

$$\|s\|_2 = \left\| X(X^*X)^{-1}X^*x_0 \right\|_2 \leq \|X\|_2 \left\| (X^*X)^{-1} \right\|_2 \|X^*x_0\|_2 \leq \sqrt{6p}\varepsilon_0 \leq \frac{\sqrt{3}}{2}.$$

Hence,

$$d^*x_0 = -\|s - x_0\|_2 = -\left(\|x_0\|_2^2 - \|s\|_2^2 \right)^{1/2} \leq -\frac{1}{2},$$

which completes the proof of the second statement. □

Proof of Theorem 2.8. Motivated by the exact property of l_1 penalty, we complete the proof by showing that any local minimizer of qL1M (2.6) actually satisfies the orthogonal constraint $X^*X = I$ and thus becomes the local minimizer of classical trace minimization method. Specifically, for any X not satisfying the orthogonal constraint, one can always find a descent direction nearby over the oblique manifold, indicating that it cannot be a local minimizer.

Denote $X = (x_1, \cdots, x_p)$. Assume that X does not satisfy the orthogonal constraint, i.e., there exists columns x_i, x_j, $i \neq j$ such that $x_i^*x_j \neq 0$. Now we find a descent direction for such X based on the value of $|x_i^*x_j|$. Given a constant $\varepsilon_0 = \frac{1}{4p}$, we divide the discussion into two scenarios.

Case 1: There exists $i, j \in \{1, \ldots, p\}$, $i \neq j$ such that $|x_i^*x_j| > \varepsilon_0$.

Without loss of generality, we assume that $|x_1^*x_2| > \varepsilon_0$. Consider a perturbation of X over oblique manifold denoted as $\widetilde{X} = (\tilde{x}_1, \cdots, \tilde{x}_p)$, such that

$$\tilde{x}_1 = \sqrt{1 - \varepsilon^2}x_1 + \varepsilon d, \quad \tilde{x}_j = x_j, \ j = 2, 3 \ldots, p,$$

with $\varepsilon > 0$ sufficiently small and $d \in \mathbb{C}^{n \times 1}$ to be determined later. Note that $p < n$, if $Ax_1 \in \mathrm{span}(X)$, there exists d such that

$$d^*d = 1, \quad d^*X = 0, \quad \text{and} \quad d^*Ax_1 = 0.$$

If $Ax_1 \notin \mathrm{span}(X)$, according to Lemma C.1, there exists d such that

$$d^*d = 1, \quad d^*X = 0, \quad \text{and} \quad d^*Ax_1 < 0.$$

In both cases we have

$$\tilde{x}_1^*\tilde{x}_1 = 1, \quad \tilde{x}_1^*\tilde{x}_j = \sqrt{1 - \varepsilon^2}x_1^*x_j, \ j = 2, \ldots, p,$$

and

$$\tilde{x}_1^* A \tilde{x}_1 = (1 - \varepsilon^2) x_1^* A x_1 + 2\varepsilon\sqrt{1 - \varepsilon^2} \mathrm{Re}(d^* A x_1) + \varepsilon^2 d^* A d.$$

Note that $\lambda_{\min}(A) \le x_1^* A x_1 \le \lambda_{\max}(A)$ and $\lambda_{\min}(A) \le d^* A d \le \lambda_{\max}(A)$, together with $d^* A x_1 \le 0$, we have

$$\begin{aligned}
E_1(\widetilde{X}) &- E_1(X) \\
&= -\varepsilon^2 x_1^* A x_1 + 2\varepsilon\sqrt{1 - \varepsilon^2} d^* A x_1 + \varepsilon^2 d^* A d + \mu_1 \sum_{j \ne 1} (\sqrt{1 - \varepsilon^2} - 1)|x_1^* x_j| \\
&\le (\lambda_{\max}(A) - \lambda_{\min}(A))\,\varepsilon^2 + \mu_1(\sqrt{1 - \varepsilon^2} - 1)\varepsilon_0 \\
&\le \left(\lambda_{\max}(A) - \lambda_{\min}(A) - \mu_1 \frac{\varepsilon_0}{2} \right) \varepsilon^2,
\end{aligned}$$

where we use $\sqrt{1 - \varepsilon^2} - 1 \le -\frac{\varepsilon^2}{2}$ for $\varepsilon > 0$ sufficiently small in the last inequality. Further, from

$$\mu_1 > 16p\|A\|_2 = \frac{4}{\varepsilon_0}\|A\|_2 \ge \frac{2}{\varepsilon_0}(\lambda_{\max}(A) - \lambda_{\min}(A)),$$

we have $E_1(\widetilde{X}) - E_1(X) < 0$, while

$$\left\| \widetilde{X} - X \right\|_{\mathrm{F}} = \left\| (\sqrt{1 - \varepsilon^2} - 1)x_1 + \varepsilon d \right\|_2 \le \varepsilon.$$

Therefore, such X cannot be a local minimizer.

Case 2: $|x_i^* x_j| \le \varepsilon_0$, *for* $i, j = 1, \ldots, p$, $i \ne j$.

Without loss of generality, we assume that $|x_1^* x_2| \ne 0$. Let $\imath = \sqrt{-1}$, denote

$$x_1^* x_2 = a + \imath b, \quad \text{where} \quad a = \mathrm{Re}(x_1^* x_2), b = \mathrm{Im}(x_1^* x_2).$$

From $(\frac{a}{\sqrt{a^2 + b^2}})^2 + (\frac{b}{\sqrt{a^2 + b^2}})^2 = 1$, we know that one of $|\frac{a}{\sqrt{a^2 + b^2}}|$ or $|\frac{b}{\sqrt{a^2 + b^2}}|$ is greater than $\frac{1}{\sqrt{2}}$. This condition further separates the discussion into two subcases.

We firstly address the case when $|\frac{a}{\sqrt{a^2 + b^2}}| \ge \frac{1}{\sqrt{2}}$. Here we assume $a = \mathrm{Re}(x_1^* x_2) > 0$, the analysis for $a < 0$ can be carried in the same manner. According to Lemma C.1, there exists $d \in \mathbb{C}^{n \times 1}$ such that

$$d^* d = 1, \quad d^* x_1 = 0, \quad d^* x_2 < -\frac{1}{2}, \quad \text{and} \quad d^* x_j = 0, \; j = 3, \ldots, p.$$

Consider a perturbation of X over oblique manifold, which is denoted as $\widetilde{X} = (\tilde{x}_1, \cdots, \tilde{x}_p)$, such that

$$\tilde{x}_1 = \sqrt{1 - \varepsilon^2} x_1 + \varepsilon d, \quad \tilde{x}_j = x_j, \; j = 2, \ldots, p.$$

Denote $c = d^* x_2 < 0$, one has

$$\begin{aligned}
\tilde{x}_1^* \tilde{x}_1 &= 1, \\
\tilde{x}_1^* \tilde{x}_2 &= \sqrt{1 - \varepsilon^2} x_1^* x_2 + \varepsilon d^* x_2 = \sqrt{1 - \varepsilon^2}(a + \imath b) + \varepsilon c, \\
\tilde{x}_1^* \tilde{x}_j &= \sqrt{1 - \varepsilon^2} x_1^* x_j, \quad j = 3, \ldots, p.
\end{aligned}$$

Note that $a > 0$, $c < 0$, let $\varepsilon > 0$ be small enough such that $\sqrt{1 - \varepsilon^2}a + \varepsilon c > 0$. Thus we have

$$|\tilde{x}_1^* \tilde{x}_2| = |\sqrt{1 - \varepsilon^2}x_1^* x_2 + \varepsilon d^* x_2| < |x_1^* x_2|.$$

Hence,

$$
\begin{aligned}
|\sqrt{1 - \varepsilon^2}x_1^* x_2 + \varepsilon d^* x_2| - |x_1^* x_2| &= \frac{|\sqrt{1 - \varepsilon^2}x_1^* x_2 + \varepsilon d^* x_2|^2 - |x_1^* x_2|^2}{|\sqrt{1 - \varepsilon^2}x_1^* x_2 + \varepsilon d^* x_2| + |x_1^* x_2|} \\
&\leq \frac{|\sqrt{1 - \varepsilon^2}x_1^* x_2 + \varepsilon d^* x_2|^2 - |x_1^* x_2|^2}{2|x_1^* x_2|} \\
&= \frac{|\sqrt{1 - \varepsilon^2}a + \varepsilon c + \imath\sqrt{1 - \varepsilon^2}b|^2 - |a + \imath b|^2}{2\sqrt{a^2 + b^2}} \\
&= \frac{1}{2\sqrt{a^2 + b^2}}\left(\varepsilon^2(c^2 - a^2 - b^2) + 2\varepsilon\sqrt{1 - \varepsilon^2}ac\right) \\
&\leq \frac{\varepsilon^2 c^2}{2\sqrt{a^2 + b^2}} + \frac{\varepsilon c}{2},
\end{aligned}
$$

where in the last equality we use $\frac{a}{\sqrt{a^2 + b^2}} \geq \frac{1}{\sqrt{2}}$ and $\sqrt{1 - \varepsilon^2} \geq \frac{1}{\sqrt{2}}$ for $\varepsilon > 0$ sufficiently small. Additionally, from

$$\tilde{x}_1^* A \tilde{x}_1 = (1 - \varepsilon^2)x_1^* A x_1 + 2\varepsilon\sqrt{1 - \varepsilon^2}\mathrm{Re}(d^* A x_1) + \varepsilon^2 d^* A d,$$

we have

$$
\begin{aligned}
E_1(\widetilde{X}) - E_1(X) &\leq -\varepsilon^2 x_1^* A x_1 + 2\varepsilon\sqrt{1 - \varepsilon^2}\mathrm{Re}(d^* A x_1) + \varepsilon^2 d^* A d \\
&\quad + \mu_1\left(\frac{\varepsilon^2 c^2}{2\sqrt{a^2 + b^2}} + \frac{\varepsilon c}{2}\right) + \mu_1 \sum_{j=3}^{p}(\sqrt{1 - \varepsilon^2} - 1)|x_1^* x_j|.
\end{aligned}
$$

Note that

$$|d^* A x_1| \leq \|d\|_2 \cdot \|A\|_2 \cdot \|x_1\|_2 \leq \|A\|_2,$$

together with $c \leq -\frac{1}{2}$ we have

$$(\text{C.2}) \qquad E_1(\widetilde{X}) - E_1(X) \leq \varepsilon\left(2\|A\|_2 - \frac{\mu_1}{4}\right) + \varepsilon^2\left(d^* A d - x_1^* A x_1 + \frac{\mu_1 c^2}{2\sqrt{a^2 + b^2}}\right).$$

Since $\mu_1 > 16p\|A\|_2$, it implies that $2\|A\|_2 - \frac{\mu_1}{4} < 0$. Besides, the right-hand side of (C.2) will be dominated by the linear term when $\varepsilon > 0$ is sufficiently small. Hence, we have $E_1(\widetilde{X}) - E_1(X) < 0$ with $\left\|\widetilde{X} - X\right\|_{\mathrm{F}} \leq \varepsilon$. Therefore, such X cannot be a local minimizer.

Now we turn to the case when $|\frac{b}{\sqrt{a^2 + b^2}}| \geq \frac{1}{\sqrt{2}}$. Without loss of generality, we assume that $b > 0$, the analysis for $b < 0$ can be carried in the same way. Again, we can find a direction d satisfying

$$d^* d = 1, \quad d^* x_1 = 0, \quad d^* x_2 < -\frac{1}{2}, \quad \text{and} \quad d^* x_j = 0, \ j = 3, \ldots, p.$$

Let $\tilde{d} = -\imath d$, then $\tilde{d}^* x_2 = \imath d^* x_2$. In the same manner, we construct a perturbation $\widetilde{X}$ of X such that

$$\tilde{x}_1 = \sqrt{1 - \varepsilon^2} x_1 + \varepsilon \tilde{d}, \quad \tilde{x}_j = x_j, \ j = 2, \ldots, p.$$

Denote $c = d^* x_2 < 0$. At this time, we have

$$\begin{aligned}
\tilde{x}_1^* \tilde{x}_1 &= 1, \\
\tilde{x}_1^* \tilde{x}_2 &= \sqrt{1 - \varepsilon^2} x_1^* x_2 + \varepsilon \tilde{d}^* x_2 = \sqrt{1 - \varepsilon^2}(a + \imath b) + \imath \varepsilon c, \\
\tilde{x}_1^* \tilde{x}_j &= \sqrt{1 - \varepsilon^2} x_1^* x_j, \quad j = 3, \ldots, p.
\end{aligned}$$

Since $b = \operatorname{Im}(x_1^* x_2) > 0$, let $\varepsilon > 0$ be small enough such that $\sqrt{1 - \varepsilon^2} b + \varepsilon c > 0$, we have

$$|\sqrt{1 - \varepsilon^2} x_1^* x_2 + \varepsilon \tilde{d}^* x_2| - |x_1^* x_2| \leq \frac{\varepsilon^2 c^2}{2\sqrt{a^2 + b^2}} + \frac{\varepsilon c}{2}.$$

Following the same discussion we have $E_1(\widetilde{X}) < E_1(X)$ with $\left\| \widetilde{X} - X \right\|_{\mathrm{F}} \leq \varepsilon$ and thus such X cannot be the local minimizer of $E_1(X)$.

We have shown that any local minimizer of qL1M satisfies the orthogonal constraint and hence is a local minimizer of classical trace minimization method,

$$\min_{X \in \mathbb{C}^{n \times p}} \operatorname{tr}(X^* A X), \quad \text{s.t.} \quad X^* X = I.$$

The analysis for the trace minimization method [37] tells that local minimizers take the form $X = Q_p V^*$, with $V \in \mathbb{C}^{p \times p}$ unitary and Q_p are eigenvectors corresponding to the p smallest eigenvalues Λ_p of matrix A. Furthermore, by substituting $X = Q_p V^*$ into the energy functional $E_1(X)$ we obtain the same objective value $E_1(Q_p V^*) = \operatorname{tr}(\Lambda_p)$. Thus, any local minimum of qL1M is also a global minimum.

On the other hand, note that oblique manifold $\mathcal{OB}(n, p)$ is a bounded and closed set and the objective function $E_1(X)$ is continuous with respect to X. Thus, qL1M must possess a global minimum over $\mathcal{OB}(n, p)$, which implies that any matrix in the form of $X = Q_p V^*$ is a global minimizer of qL1M and there are no other local minimizers. □

REFERENCES

[1] D. S. Abrams and S. Lloyd, *Quantum algorithm providing exponential speed increase for finding eigenvalues and eigenvectors*, Physical Review Letters, 83 (1999), p. 5162.

[2] F. Arute, K. Arya, R. Babbush, D. Bacon, J. C. Bardin, R. Barends, R. Biswas, S. Boixo, F. G. Brandao, D. A. Buell, et al., *Quantum supremacy using a programmable superconducting processor*, Nature, 574 (2019), pp. 505–510.

[3] A. Aspuru-Guzik, A. D. Dutoi, P. J. Love, and M. Head-Gordon, *Simulated quantum computation of molecular energies*, Science, 309 (2005), pp. 1704–1707.

[4] B. Bauer, S. Bravyi, M. Motta, and G. K.-L. Chan, *Quantum algorithms for quantum chemistry and quantum materials science*, Chemical Reviews, 120 (2020), pp. 12685–12717.

[5] J. Bierman, Y. Li, and J. Lu, *Quantum orbital minimization method for excited states calculation on a quantum computer*, Journal of Chemical Theory and Computation, 18 (2022), pp. 4674–4689.

[6] N. Blunt, S. D. Smart, G. H. Booth, and A. Alavi, *An excited-state approach within full configuration interaction quantum Monte Carlo*, The Journal of Chemical Physics, 143 (2015).

[7] H. Chen and Y. Li, *On the continuity of Schur-Horn mapping*, arXiv preprint arXiv:2407.00701, (2024).

[8] J. I. Colless, V. V. Ramasesh, D. Dahlen, M. S. Blok, M. E. Kimchi-Schwartz, J. R. McClean, J. Carter, W. A. de Jong, and I. Siddiqi, *Computation of molecular spectra on a quantum processor with an error-resilient algorithm*, Physical Review X, 8 (2018), p. 011021.

[9] P. Deglmann, A. Schäfer, and C. Lennartz, *Application of quantum calculations in the chemical industry—an overview*, International Journal of Quantum Chemistry, 115 (2015), pp. 107–136.

[10] M. Ganzhorn, D. J. Egger, P. Barkoutsos, P. Ollitrault, G. Salis, N. Moll, M. Roth, A. Fuhrer, P. Mueller, S. Woerner, et al., *Gate-efficient simulation of molecular eigenstates on a quantum computer*, Physical Review Applied, 11 (2019), p. 044092.

[11] W. Gao, Y. Li, and H. Shen, *Weighted trace-penalty minimization for full configuration interaction*, SIAM Journal on Scientific Computing, 46 (2024), pp. A179–A203.

[12] H. R. Grimsley, S. E. Economou, E. Barnes, and N. J. Mayhall, *An adaptive variational algorithm for exact molecular simulations on a quantum computer*, Nature communications, 10 (2019), p. 3007.

[13] O. Higgott, D. Wang, and S. Brierley, *Variational quantum computation of excited states*, Quantum, 3 (2019), p. 156.

[14] A. A. Holmes, C. Umrigar, and S. Sharma, *Excited states using semistochastic heat-bath configuration interaction*, The Journal of Chemical Physics, 147 (2017).

[15] A. Javadi-Abhari, M. Treinish, K. Krsulich, C. J. Wood, J. Lishman, J. Gacon, S. Martiel, P. D. Nation, L. S. Bishop, A. W. Cross, et al., *Quantum computing with Qiskit*, arXiv preprint arXiv:2405.08810, (2024).

[16] T. Jones, S. Endo, S. McArdle, X. Yuan, and S. C. Benjamin, *Variational quantum algorithms for discovering Hamiltonian spectra*, Physical Review A, 99 (2019), p. 062304.

[17] A. Kandala, A. Mezzacapo, K. Temme, M. Takita, M. Brink, J. M. Chow, and J. M. Gambetta, *Hardware-efficient variational quantum eigensolver for small molecules and quantum magnets*, nature, 549 (2017), pp. 242–246.

[18] A. Y. Kitaev, *Quantum measurements and the Abelian stabilizer problem*, arXiv preprint quant-ph/9511026, (1995).

[19] J. Lee, W. J. Huggins, M. Head-Gordon, and K. B. Whaley, *Generalized unitary coupled cluster wave functions for quantum computation*, Journal of chemical theory and computation, 15 (2018), pp. 311–324.

[20] Y. Li and J. Lu, *Optimal orbital selection for full configuration interaction (OptOrbFCI): Pursuing the basis set limit under a budget*, Journal of Chemical Theory and Computation, 16 (2020), pp. 6207–6221.

[21] Y. Li, J. Lu, and Z. Wang, *Coordinate-wise descent methods for leading eigenvalue problem*, SIAM Journal on Scientific Computing, 41 (2019), pp. A2681–A2716.

[22] X. Liu, Z. Wen, and Y. Zhang, *An efficient Gauss–Newton algorithm for symmetric low-rank product matrix approximations*, SIAM Journal on Optimization, 25 (2015), pp. 1571–1608.

[23] J. Lu and K. Thicke, *Orbital minimization method with ℓ_1 regularization*, Journal of Computational Physics, 336 (2017), pp. 87–103.

[24] F. Mauri, G. Galli, and R. Car, *Orbital formulation for electronic-structure calculations with linear system-size scaling*, Physical Review B, 47 (1993), p. 9973.

[25] S. McArdle, S. Endo, A. Aspuru-Guzik, S. C. Benjamin, and X. Yuan, *Quantum computational chemistry*, Reviews of Modern Physics, 92 (2020), p. 015003.

[26] J. R. McClean, M. E. Kimchi-Schwartz, J. Carter, and W. A. De Jong, *Hybrid quantum-classical hierarchy for mitigation of decoherence and determination of excited states*, Physical Review A, 95 (2017), p. 042308.

[27] J. R. McClean, J. Romero, R. Babbush, and A. Aspuru-Guzik, *The theory of variational hybrid quantum-classical algorithms*, New Journal of Physics, 18 (2016), p. 023023.

[28] K. M. Nakanishi, K. Mitarai, and K. Fujii, *Subspace-search variational quantum eigensolver for excited states*, Physical Review Research, 1 (2019), p. 033062.

[29] J. Nocedal and S. J. Wright, *Numerical optimization*, Springer, 1999.

[30] P. J. Ollitrault, A. Kandala, C.-F. Chen, P. K. Barkoutsos, A. Mezzacapo, M. Pistoia, S. Sheldon, S. Woerner, J. M. Gambetta, and I. Tavernelli, *Quantum equation of motion for computing molecular excitation energies on a noisy quantum processor*, Physical Review Research, 2 (2020), p. 043140.

[31] P. Ordejón, D. A. Drabold, M. P. Grumbach, and R. M. Martin, *Unconstrained minimization approach for electronic computations that scales linearly with system size*, Physical Review B, 48 (1993), p. 14646.

[32] R. M. Parrish, E. G. Hohenstein, P. L. McMahon, and T. J. Martínez, *Quantum computation of electronic transitions using a variational quantum eigensolver*, Physical review letters, 122 (2019), p. 230401.

[33] A. Peruzzo, J. McClean, P. Shadbolt, M.-H. Yung, X.-Q. Zhou, P. J. Love, A. Aspuru-Guzik, and J. L. O'brien, *A variational eigenvalue solver on a photonic quantum processor*, Nature communications, 5 (2014), p. 4213.

[34] J. Preskill, *Quantum computing in the NISQ era and beyond*, Quantum, 2 (2018), p. 79.

[35] J. Romero, R. Babbush, J. R. McClean, C. Hempel, P. J. Love, and A. Aspuru-Guzik, *Strategies for quantum computing molecular energies using the unitary coupled cluster ansatz*, Quantum Science and Technology, 4 (2018), p. 014008.

[36] I. G. Ryabinkin, T.-C. Yen, S. N. Genin, and A. F. Izmaylov, *Qubit coupled cluster method: a systematic approach to quantum chemistry on a quantum computer*, Journal of chemical theory and computation, 14 (2018), pp. 6317–6326.

[37] A. H. Sameh and J. A. Wisniewski, *A trace minimization algorithm for the generalized eigenvalue problem*, SIAM Journal on Numerical Analysis, 19 (1982), pp. 1243–1259.

[38] R. Santagati, J. Wang, A. Gentile, S. Paesani, N. Wiebe, J. McClean, D. Bonneau, J. Silverstone, S. Morley-Short, P. Shadbolt, et al., *Finding excited states of physical Hamiltonians on a silicon quantum photonic device*, in Frontiers in Optics, Optica Publishing Group, 2017, pp. FM4E–2.

[39] R. Santagati, J. Wang, A. A. Gentile, S. Paesani, N. Wiebe, J. R. McClean, S. Morley-Short, P. J. Shadbolt, D. Bonneau, J. W. Silverstone, et al., *Witnessing eigenstates for quantum simulation of Hamiltonian spectra*, Science advances, 4 (2018), p. eaap9646.

[40] J. B. Schriber and F. A. Evangelista, *Adaptive configuration interaction for computing challenging electronic excited states with tunable accuracy*, Journal of chemical theory and computation, 13 (2017), pp. 5354–5366.

[41] Q. Sun, T. C. Berkelbach, N. S. Blunt, G. H. Booth, S. Guo, Z. Li, J. Liu, J. D. McClain, E. R. Sayfutyarova, S. Sharma, S. Wouters, and G. K.-L. Chan, *PySCF: the Python-based simulations of chemistry framework*, Wiley Interdisciplinary Reviews: Computational Molecular Science, 8 (2018), p. e1340.

[42] J. Tilly, H. Chen, S. Cao, D. Picozzi, K. Setia, Y. Li, E. Grant, L. Wossnig, I. Rungger, G. H. Booth, and J. Tennyson, *The variational quantum eigensolver: a review of methods and best practices*, Physics Reports, 986 (2022), pp. 1–128.

[43] Z. Wang, Y. Li, and J. Lu, *Coordinate descent full configuration interaction*, Journal of chemical theory and computation, 15 (2019), pp. 3558–3569.

[44] Z. Wen, C. Yang, X. Liu, and Y. Zhang, *Trace-penalty minimization for large-scale eigenspace computation*, Journal of Scientific Computing, 66 (2016), pp. 1175–1203.

[45] H.-S. Zhong, H. Wang, Y.-H. Deng, M.-C. Chen, L.-C. Peng, Y.-H. Luo, J. Qin, D. Wu, X. Ding, Y. Hu, et al., *Quantum computational advantage using photons*, Science, 370 (2020), pp. 1460–1463.